Reduction of Nitro Aromatic Compounds in Fe^0-CO_2-H_2O Systems: Implications for Groundwater Remediation with Iron Metal

Abinash Agrawal
Ph.D. in Geology
University of North Carolina at Chapel Hill, 1990

A thesis submitted to the faculty of the
Oregon Graduate Institute of Science & Technology
in partial fulfillment of
the requirements for the degree
Master of Science in
Environmental Science and Engineering

July 1995

The dissertation "Reduction of Nitro Aromatic Compounds in Fe^0-CO_2-H_2O Systems: Implications for Groundwater Remediation with Iron Metal" by Abinash Agrawal has been examined and approved by the following Examination Committee:

Paul G. Tratnyek, Thesis Advisor
Assistant Professor

Carl D. Palmer
Associate Professor

Richard L. Johnson
Associate Professor

Acknowledgements

This graduate research would not have been possible without the vision and support of my advisor, Dr. Paul G. Tratnyek. Paul was extremely helpful and encouraging at every stage of the work. I gratefully express thanks to Mark A. Williamson (PDF Advisor), Atlantic Geoscience Centre, Geological Survey of Canada, for support and encouragement during thesis preparation, while I was a Visiting Postdoctoral Fellow of the National Science and Engineering Research Council (Energy, Mines and Resources), Canada. I must sincerely acknowledge the support of my wife, Ranjana, and our son, Ravi, who stood by me during the difficult months.

This study was supported in part by the University Consortium Solvent-In-Groundwater Research Program, the U.S. Environmental Protection Agency through Cooperative Agreement CR 82078-01-0, and the National Science Foundation through Award BCS-9212059. This has not been subject to review by the U.S. Environmental Protection Agency and therefore does not necessarily reflect the views of the Agency and no official endorsement should be inferred.

Table of Contents

List of figures

List of tables

Abstract

Reduction of Nitro Aromatic Compounds in Fe^0-CO_2-H_2O Systems: Implications for Groundwater Remediation with Iron Metal

The properties of iron metal that make it useful in remediation of chlorinated solvents may also lead to reduction of other groundwater contaminants such as nitro aromatic compounds (NACs). This possibility has been investigated in batch experiments using aqueous carbonate media to determine the kinetics and mechanism of nitro reduction by iron metal, and to learn more about the effect of precipitation on the reactivity of the metal surfaces under geochemical conditions. Nitrobenzene is reduced by iron under anaerobic conditions to aniline with nitrosobenzene as an intermediate product. Detectable amounts of coupling products such as azobenzene and azoxybenzene were not found. First-order reduction rates are similar for nitrobenzene and nitrosobenzene, but aniline appearance occurs more slowly (typical pseudo first-order rate constants 3.5×10^{-2}, 3.4×10^{-2}, and 8.8×10^{-3} min^{-1}, respectively, in the presence of 33 g/L of acid-washed, 18-20 mesh Fluka iron turnings). The nitro reduction rate increased linearly with concentration of iron surface area, giving a specific reaction rate constant ($3.9 \pm 0.2 \times 10^{-2}$ min^{-1} m^{-2} L) which is roughly 16-fold greater than has been reported for dehalogenation of carbon tetrachloride. A linear correlation was also observed between nitrobenzene reduction rate constants and the square-root of mixing rate (rpm), suggesting that the observed reaction rates were controlled by mass transfer of the NAC to the metal surface. Further evidence for diffusion control was found in the minimal effects of solution pH or ring substitution on nitro reduction. Scanning electron microscopy with energy-dispersive X-ray spectroscopy supported by XRD analysis of the metal surface confirmed that dissolved carbonate concentrations typical of natural groundwaters ($\approx 10^{-2}$ *M*) produced a siderite ($FeCO_3$) film on the metal surface. The decrease in reduction rate for nitrobenzene with increased concentration of dissolved carbonate, and with extended exposure of the metal to a particular carbonate buffer, indicate that the precipitation of siderite on the metal inhibits nitro reduction, presumably by limiting mass transfer of reactant(s) to the surface.

Chapter 1

Introduction

Over the last several years, a great deal of interest has developed in the groundwater remediation community over the prospects of new treatment strategies based on dechlorination by granular iron metal. The apparent success of the first field demonstration[1] at Base Borden, Ontario, has led to initiation of numerous feasibility studies, pilot tests, and small to medium scale demonstration projects.[2,3] These developments have created a need for more process-level insight into the chemistry of these systems in order to explain, predict, and/or enhance their performance.

The first detailed studies of halocarbon degradation by iron metal in laboratory batch systems[4,5] made several fundamental considerations apparent: (i) halocarbon degradation occurs by dechlorination through a surface reaction with the metal as the ultimate electron donor; (ii) the major determinants of degradation kinetics are mass transfer to, area of, and condition of the metal surface; and (iii) other factors may influence the rate of reaction, however mediation by H_2, Fe^{2+}, metal impurities, or microorganisms do not appear to be necessary for rapid degradation. Concurrent studies performed in laboratory columns[5,6] showed that halocarbon degradation occurs similarly in porous media, but that there is an important additional consideration: geochemical evolution of the matrix material by iron dissolution and precipitation over the course of extended operation. Many additional studies of contaminant remediation with zero-valent metals have now been reported.[2,7-9] These studies support the view that contaminant degradation results from reduction coupled to: metal corrosion, and most address at least one additional factor, such as the range of contaminants that may be remediated with reducing metals, the effect of groundwater geochemistry on remediation performance, or the possibilities for enhanced performance with derivative technologies. In this study, we investigated the reduction of nitrobenzene by iron metal in carbonate-buffered batch systems to (i) assess the potential utility of nitro reduction by Fe^0 in groundwater remediation, (ii) further our understanding of the reactivity of Fe^0 with organic solutes in

aqueous systems, and (iii) gain insight into the role that precipitation of solids such as $FeCO_3$ may play in remediation performance under geochemical conditions.

The remediation of nitro aromatic compounds (NACs) is of interest because the nitro aromatic moiety is among the most characteristic of anthropogenic contaminants, being second only to organochlorine functional groups. NACs are common environmental contaminants because of their use as munitions, insecticides, herbicides, pharmaceuticals, and industrial feed stock chemicals for dyes, plastics, etc.[10] They also may be formed in the environment from aromatic contaminants, as is the case with the nitro-PAHs and nitrophenols found in atmospheric waters.[11,12] Among the processes contributing to the environmental fate of NACs,[13] reduction of the nitro group is certainly the most characteristic. The transformation reaction generally produces the corresponding aromatic amines, with minor amounts of intermediates (hydroxylamines and nitroso compounds) and coupling products (azo and azoxy compounds). Of course, aromatic amines are still of concern as environmental contaminants, so remediation of NACs requires transformation beyond nitro reduction. Two possible treatments for making nitro reduction products completely innocuous are: (i) biodegradation, which sometimes occurs more rapidly for aromatic amines than for the parent nitro compounds[14] and (ii) incorporation into natural organic matter by enzyme-catalyzed coupling reactions.[15] In principle, either technique could be coupled to nitro reduction with Fe^0, and the combination applied to remediate environmental contamination by NACs.

Beyond the direct relevance of nitro reduction to remediation objectives, the reaction was also selected for its advantages as a probe technique with which to study the behavior of Fe^0 in geochemical systems. For this purpose, nitroaromatic reduction offers three important advantages over dechlorination: (i) volatilization of the organic reactant and its reduction products are much less of a concern, (ii) the specific rate of reaction is more rapid, and (iii) the reaction products do not include chloride, which itself is a strong promoter of corrosion. In part due to these advantages, exceptionally reproducible rates of contaminant reduction were obtained in this study. The experiments were conducted in CO_2-buffered solutions to control pH and to simulate interactions between carbonate species and Fe^0. Of the possible interactions between dissolved CO_2 and Fe^0, precipitation of iron carbonate was of particular concern because of its potential to interfere with remediation performance in the field by passivating iron surfaces. The model systems used in this study produced grains of Fe^0 coated with varying amounts of

iron carbonate, and have allowed us to investigate the role of precipitates in mediating contaminant degradation.

Chapter 2

Background

2.1 Oxidation of Fe^0

Zero-valent iron metal, Fe^0, is readily oxidized to ferrous iron, Fe^{2+}, by many substances. In aqueous systems, this phenomenon leads to dissolution of the solid, which is the primary cause of metal corrosion. Metal corrosion is an electrochemical process, in which oxidation of Fe^0 to Fe^{2+} is the anodic half-reaction. The associated cathodic reaction may vary with the reactivity of available electron acceptors. In anoxic pure aqueous media, the acceptors include H^+ and H_2O, the reduction of which yields OH^- and H_2. Thus, the overall process of corrosion in anaerobic Fe^0-H_2O systems is classically described by the following reactions.

$$Fe^0 + 2\ H^+ \rightleftharpoons Fe^{2+} + H_2 \quad (1)$$

$$Fe^0 + 2\ H_2O \rightleftharpoons Fe^{2+} + H_2 + 2\ OH^- \quad (2)$$

The preferred cathodic half-reaction under aerobic conditions involves O_2 as the electron acceptor. In this case, the primary reaction yields only OH^- and not H_2.

$$2\ Fe^0 + O_2 + 2\ H_2O \rightleftharpoons 2\ Fe^{2+} + 4\ OH^- \quad (3)$$

Other strong electron acceptors (oxidants) may offer additional cathodic reactions that contribute to iron corrosion. For example, systems containing HCO_3^- and H_2CO_3 species may oxidize Fe^0 and promote corrosion (eqs 5-6). Organic oxidants also can react with Fe^0, as illustrated by the dehalogenation of chlorinated hydrocarbons, RCl.

$$Fe^0 + RCl + H^+ \rightleftharpoons Fe^{2+} + RH + Cl^- \quad (4)$$

Reaction 4 can contribute significantly to the net dissolution of iron, even in predominantly aqueous systems.[16] The utility of this reaction has long been recognized

in organic synthesis, and more recently in environmental remediation.[4,5] NACs also exhibit facile reduction by Fe^0 but this reaction is not a significant contributor to material damage by corrosion, and therefore has not been studied in detail from the corrosion perspective.

The factors affecting rates of metal corrosion have been studied extensively.[17,18] At a clean surface, low pH and the presence of strong oxidants favor fast corrosion. However, the accumulation of inert reaction products on the metal surface eventually causes the corrosion rate to decrease, resulting in the phenomenon known as passivation. Reaction products that contribute to passivity include metal oxides, carbonates, and gaseous H_2. All of the oxidants that contribute to corrosion, can further oxidize Fe^{2+} to Fe^{3+}, which leads to precipitation of amorphous and crystalline forms of ferric oxyhydroxides (e.g., γ-FeOOH) and the eventual accumulation of rust. The layer of solid products at the surface limits mass-transport to and/or from the reactive sites of the metal. The reverse phenomenon, depassivation, results from: (i) chemical destabilization of uniform passive films by aggressive anions, particularly chloride and sulfide,[19-21] (ii) localization of anodic dissolution at surface defects, which eventually develop into corrosion pits,[22] and (iii) renewal of the active metal surface by physical processes such as abrasion.[23,24] Depassivation allows increased rates of cathodic reaction at the metal surface and, therefore, should benefit the application of Fe^0 in environmental remediation.

2.2 Corrosion in the Fe^0-H_2O-CO_2 System

The effects of carbonate species on iron metal corrosion have been studied extensively due to the frequent occurrence of slightly acidic, anaerobic, CO_2-rich formation waters and condensates in oil and gas production.[25] It is now well established that dissolved CO_2 can accelerate iron corrosion, while significant precipitation of $FeCO_3$ results in passivation. Although the exact mechanism of corrosion acceleration by carbonate is still the subject of investigation,[26,27] it is clear that adsorbed H_2CO_3 and HCO_3^- react as oxidants, providing two cathodic reactions to drive metal dissolution in addition to eqs 1 and 2.[26,28,29]

$$Fe^0 + 2\ H_2CO_{3\ (ads)} \rightleftharpoons Fe^{2+} + 2\ HCO_{3\ (ads)}^- + H_2\ (g) \qquad (5)$$

$$Fe^0 + 2\ HCO_{3\ (ads)}^- \rightleftharpoons Fe^{2+} + 2\ CO_{3\ (ads)}^{2-} + H_2\ (g) \qquad (6)$$

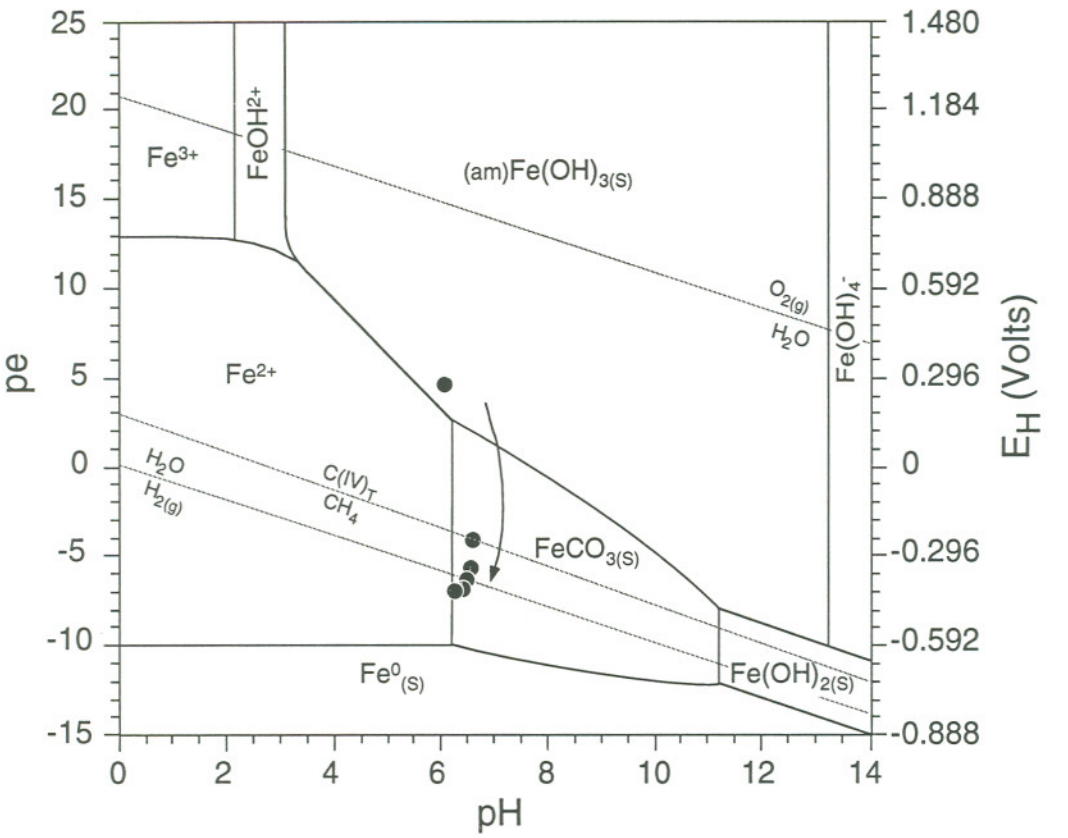

Figure 2.1: Eh-pH diagram for the Fe^0-H_20-CO_2 system with 10^{-4} *M* total iron and 1.5 x 10^{-2} *M* total carbonate, neglecting activity corrections. Below the $C(IV)_T/CH_4$ line, all the Eh-pH lines involving $FeCO_3$ assume that total dissolved carbonate is present at a constant level at 1.5 x 10^{-2} *M* (i.e., is not reduced by the metal). Fe_2O_3 and Fe_3O_4 species are not included because slow kinetics may not allow their formation in our model systems, as a typical experiment ran for 4-5 hr.[32,78] The data points (measured periodically over 5 days) and arrow indicate trend in Eh-pH evolution due to corrosion and $FeCO_3$(s) formation, during an extended incubation of Fe^0 in bicarbonate medium.

Equilibration with water restores the original carbonate speciation, and the net result of eqs 5 and 6 is catalysis of H_2 evolution by iron corrosion mediated by carbonate. In addition, the thermodynamic potential of Fe^0 is sufficiently strong to reduce the C(+IV) of carbonate species to the C(-IV) of hydrocarbons (Figure 2.1). Although this reaction is widely believed to be insignificant due to kinetic limitations, it is well documented in experiments where large negative potentials are imposed at metal electrodes,[30] and apparently also occurs to a measurable degree on iron metal surfaces even without an imposed potential.[31]

In Fe^0-H_2O-CO_2 systems, the Fe^{2+} produced by corrosion can precipitate as carbonates as well as oxides. Figure 2.1 shows the metastable species that are expected under conditions relevant to this study (total dissolved Fe =10^{-5} *M*; total dissolved carbonate = 1.5 x 10^{-2} *M*). Oxidation of Fe^0 yields predominantly $FeCO_{3\,(s)}$ at pH ~ 6-11 and $Fe(OH)_{2\,(s)}$ at pH >11. In a traditional equilibrium analysis of corrosion potentials,[32] conditions that favor formation of $FeCO_{3\,(s)}$, $Fe(OH)_{2\,(s)}$, and $Fe(OH)_{3\,(s)}$ should passivate the metal, whereas sustained corrosion is expected only below pH 6 where the product is aqueous Fe^{2+}. However, application of this analysis to the present study is complicated due to supersaturation with respect to iron carbonates, which is frequently observed under environmental conditions.[33] This phenomenon is reflected in the slow kinetics of $FeCO_{3\,(s)}$ precipitation,[34,35] and formation of stable aqueous $FeCO_3^0$ and $Fe(CO_3)_2^{2-}$ complexes.[33] Since $FeCO_3$ is unlikely to contribute to reduction of contaminants, we expect the degree to which carbonate precipitates coat Fe^0 surfaces under environmental conditions will be an important determinant of potential remediation performance.

2.3 Chemical Transformations of NACs

Under reducing conditions, NACs may react by a variety of pathways, which are summarized in Figure 2.2. Most of these reactions have been studied in great detail either as preparative methods in synthetic chemistry, or model reactions for electrochemical investigations, and numerous reviews on these topics are available.[36-42] In almost all cases, the major process is reduction of the nitro functional group to the corresponding amine (Figure 2.2, Reactions I-III). Formally, this process consists of a series of two-electron additions, proceeding through nitroso and hydroxylamine intermediates. However, the reduction potentials for reactions I and II are very similar (Table 2.1), so polarography performed on acid to neutral aqueous solutions gives only two waves: the

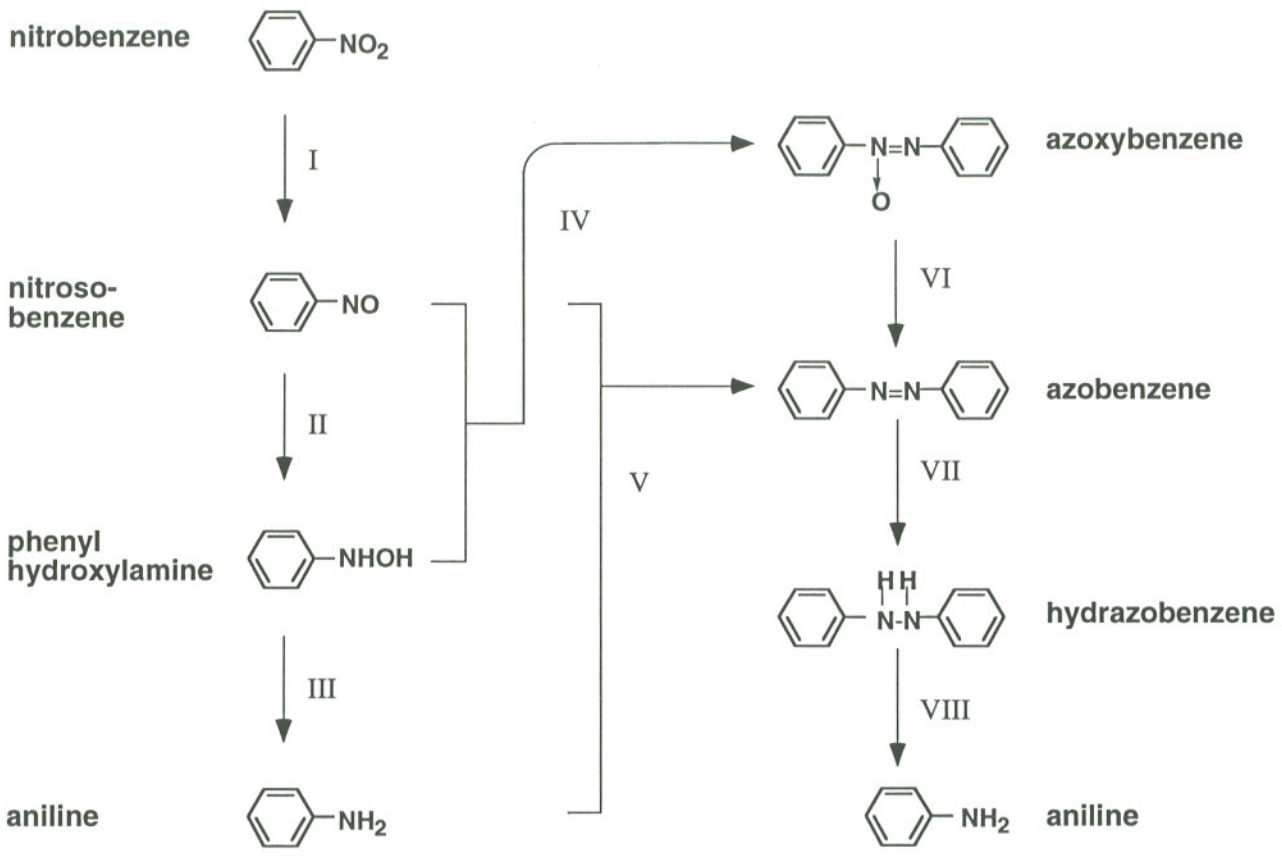

Figure 2.2: Schematic diagram showing the various possible transformation pathways for nitrobenzene in reducing environments. Downward arrows (reactions I-III and VI-VII) indicate reduction reactions and right-facing arrows (reactions IV-V) indicate condensations. The dominant reduction pathway of the nitro group to its amino equivalent may occur sequentially via nitroso and hydroxylamine (reaction I-III).

Table 2.1. Properties of Nitrobenzene and its reduction products §.

Compound	D (cm^2 s^{-1}) †	$E_{1/2}$ (V vs NHE) ¥	pK_a
Nitrobenzene	6.8×10^{-6}	-0.55[37]	
Nitrosobenzene	7.1×10^{-6}	-0.63[38]	-4.9[63]
Phenylhydroxylamine	6.9×10^{-6}	-1.29[73]	3.2[74]
Aniline	7.2×10^{-6}		4.6[75]

§ All data for aqueous or nearly aqueous solution. Sources are referenced as superscripts.

† Molecular diffusivity estimated for 15°C after Tucker and Nelken.[76]

¥ Polarographic half-wave potentials for aqueous solution at pH 7.

first corresponding to a four-electron reduction for formation of the hydroxylamine, and the second corresponding to a two-electron reduction of the hydroxylamine to the amine. At alkaline pH, only one six-electron wave is observed. Accumulation of the nitroso compound is rarely found in practice, and special techniques are often necessary to obtain direct evidence for its formation.[43,44] Indirect evidence for its formation is abundant, however, because condensation reactions involving the nitroso intermediate (Reactions IV-V) give azoxy and azo compounds, which are frequently observed in significant yields from nitro reduction.[45-47] Product distributions may be further complicated by reduction of the condensation products (Reactions VI-VII)[48] or rearrangements such as the formation of benzidine (not shown).[49]

Reduction of NACs is well documented for aqueous media containing metals such as Fe, Zn, or Sn because these reactions have been used widely in the synthesis of amines.[50] According to a method that originated with an early study by Lyons and Smith,[51] high yields can be obtained using Fe^0 and trace amounts of salts containing Fe^{2+} or Cl^-. In addition to the formation of amines, dissolving metal reductions of NACs may produce good yields of the other products represented in Figure 2.2. For example, reduction of nitrobenzene with Zn is reported to be useful for preparation of phenylhydroxylamine.[52] In general, however, yields of products other than the amines are usually small and variable, so the reaction is of limited synthetic utility and has received little attention in the recent literature.

In environmental media, reduction of NACs occurs by both biotic and abiotic means.[53] The dominant reaction pathway under anaerobic environmental conditions appears to be nitro reduction to the amine. However, there is evidence for most of the other pathways in Figure 2.2, including coupling of nitro reduction intermediates to form azo and azoxy compounds, and reductive cleavage of azo compounds to form amines.[54] The former reaction is of particular importance because azo and azoxy compounds are of greater concern as environmental contaminants than their precursors. The aromatic amines formed by nitro reduction, are subject to additional reactions in environmental systems including covalent binding to natural organic matter[55] or specific adsorption to mineral surfaces.[56] In addition to the reactions included in Figure 2.2, environmental transformation of NACs can include further degradation by microorganisms. This is likely to include hydroxylation and cleavage of the aromatic ring with eventual mineralization, but such reactions are not expected by the direct action of reducing metals alone.

Chapter 3

Experimental Section

3.1 Chemicals

Nitro aromatic compounds and their likely reaction products were obtained in high purity and used as received. These included nitrobenzene, 1-chloro-4-nitrobenzene, 1,3-dinitrobenzene, 4-nitrotoluene, 4-nitroanisole, 2,4,6-trinitrotoluene, parathion, nitrosobenzene, aniline, azobenzene, and azoxybenzene. Roughly mM-stock solutions were prepared in deionized water (18 MW-cm NANOpure) with up to 5% (v/v) HPLC-grade methanol. Buffers used included 2-(*N*-cyclohexylamino)ethanosulfonic acid (CHES); *N*-(2-morpholino)ethane-sulfonic acid (MES); *N*-(2-hydroxyethyl)-piperazine-*N'*-2-ethanesulfonic acid (HEPES); 3-(*N*-morpholino)propanesulfonic acid (MES); and tris(hydroxymethyl)aminomethane (TRIS). Analytical grade CO_2 and other gases were deoxygenated prior to use by passing through a heated column of reduced copper.

The iron metal used in this study (Fluka electrolytic iron, Catalog #44905) was selected to give manageable nitro reduction rates in the experimental system described below. Compared with the Fe^0 used in most other studies,[4,6] this material has a coarser grain size (mostly >40 mesh) and clean, smooth surfaces with a high metallic luster. The nominal purity is 99.9% with the remainder consisting primarily of iron oxide. Trace impurities are less than 0.02% C, 0.008% S, 0.003% Si, 0.002% P, 0.002% Mn, and 5 ppm Mg. The surface area of a sieved iron sample prior to acid-treatment was determined to be 0.005 m^2/g by gas adsorption using BET analysis.

3.2 Iron pretreatment

Prior to use, the Fe^0 grains were hand-sieved to constrain grain size to 18-20 mesh and sonicated in 10% HCl (v/v) for 20 min to remove surface oxides or other contaminants. The cleaned metal was washed 4 times with the bicarbonate buffer to

remove residual acidity or chloride from the acid treatment. The entire acid-washing procedure was performed under a stream of deoxygenated N_2 with freshly deoxygenated bicarbonate buffer to avoid further surface oxidation to metal oxides. A series of control tests indicated that the mass of Fe^0 lost due to this pretreatment was 4.86±0.2%. The BET surface area of the iron sample following the acid-treatment increased to 0.038 m^2/g.

3.3 Buffer formulation

The bicarbonate buffer media were prepared by flowing deoxygenated 1% CO_2 in N_2 or 100% CO_2 (i.e., $pCO_2 = 0.01$ and 1.0 atm respectively) for roughly 2 hr through a 15 mM NaOH solution in deionized water. The pH range available from the above method was between 5.5 and 8.0, as determined by pCO_2 and the aqueous alkalinity. To prepare more acidic buffers, the initial NaOH solution was modified by addition of 10% HCl (v/v) prior to sparging with CO_2.

3.4 Model reaction systems

Individual degradation experiments were performed in anaerobic (sealed) batch systems prepared in 60-mL serum bottles. In most cases, bottles received 2 g of sieved iron, weighed dry to the nearest mg prior to acid treatment. Following the acid-wash, the bottles were filled with fresh bicarbonate buffer medium and crimp-sealed using thick butyl rubber septa (Pierce). During this procedure, the headspace of each bottle was purged with the same gas used for buffer preparation (deoxygenated 1% CO_2 in N_2 or 100% CO_2). Any gas bubbles that remained after capping, were displaced with buffer medium using a pair of needles through the septum. Before initiating degradation experiments, each bottle was allowed 2 hr to equilibrate on an end-over-end rotary shaker at 10 rpm in a dark, 15 °C room.

A typical reduction experiment began by addition of 1 mL of 10^{-3} *M* deoxygenated aqueous stock solution of nitrobenzene (or nitrosobenzene, or one of the substituted nitrobenzenes) by needle injection through the septum. A second needle was used to allow an equal volume of fluid to be displaced, so each experiment began at 1 atm pressure and without headspace. Standard incubation conditions were maintained throughout each experiment (i.e., dark, 15°C, 10 rpm). Loss of parent organic compound and formation of reduction products were determined by periodically removing 200 µL

samples for immediate analysis by HPLC. As the sample was withdrawn from the bottle the resulting negative pressure was relieved by allowing deoxygenated N_2 to enter through a second needle. The BET surface area of the iron sample obtained from serum bottles after the reduction experiment was 0.021 m^2/g.

3.5 Analyses

The concentrations of unreacted substrate and its various reaction products were determined by isocratic HPLC with UV absorbance detection. The analytical column (4 mm x 10 cm) consisted of Microsorb packing (particle size, 3 mm) with a C-18 stationary phase. A precolumn (4.6 mm x 1.5 cm) of the same material was also used. The eluent consisted of 60/40 acetonitrile and water with a flow-rate of 0.9 mL/min. The absorbance was monitored at 270 nm, which is close to the λ_{max} for nitrobenzene (272 nm) and nitrosobenzene (280, 300 nm). Peaks were identified by comparison with the retention times of standard compounds and concentrations were determined from peak areas by comparison to standard curves.

The Fe^0 surface was characterized in terms of surface area and morphology at various stages of our experiments. Surface area was estimated by BET Kr-gas adsorption (Micromeritics Instruments, Inc.) on samples that were prepared by rapidly drying the metal with methanol and storing under N_2 to avoid surface oxidation. Surface morphology was determined by scanning electron microscopy (SEM) using an Environmental SEM (Electroscan) with energy-dispersive X-ray spectroscopy (EDS). The digital SEM images were obtained at an accelerating voltage of 10-20 kV, using a Si(Li) source with a working distance of 11-13 mm. The EDS was performed at a take-off angle of 4-6 degrees.

Measurements of Pt electrode potential and pH of the aqueous medium were made during several experiments with a combination, needle-form Pt electrode (18 gauge beveled-tip, Microelectrodes, Inc.) pierced through the septum of sealed (anaerobic) serum bottles. Measurements following the experiment were made in open bottles with a gel-filled combination electrode. All electrode potentials are reported in mV versus the standard hydrogen electrode (SHE).

Chapter 4

Results and Discussion

4.1 Model system design and characterization

An important element of this study was to refine and improve on the experimental protocol used in previous work.[4] The original protocol was developed to give a rapid and convenient method for studying the effects of reaction variables on the reduction of organic substrates by Fe^0. The method involves batch experiments conducted without headspace, but with continuous mixing under controlled conditions and selected amounts of high-purity, acid-cleaned Fe^0. Preliminary results in this study confirmed that reproducibility is improved by (i) constraining Fe grain size by sieving and (ii) pretreating iron surfaces with dilute HCl. The addition of carbonate to buffer pH and focus on NACs, also seem to have contributed to improved reproducibility of substrate reduction rates. Using the protocol developed in this study, the average standard deviation for nitro reduction rate constants determined for several series of replicate experiments was <2.5%.

Early experiments in unbuffered Fe-H_2O systems resulted in the expected pH rise (>2 units in ~4 hr) due to aqueous corrosion of the metal (eqs 2-3). This change in pH over the course of a typical experiment could influence the observed kinetics of substrate reduction by several mechanisms, including the direct participation of H^+ as a reactant (e.g., as in eq 4) and passivation of the metal toward corrosion by precipitation of metal oxyhydroxides and carbonates. Although previous batch studies of dechlorination by Fe^0 have not shown evidence that the pH rise due to aqueous corrosion significantly effects contaminant degradation rates,[4] we favored buffered systems for this study to gain greater control over experimental conditions. Previous studies have used various biological buffers in batch systems containing Fe^0 and not found any specific buffer effects.[4,7,8] However, our control experiments showed visible precipitation in only a few hours with as little as 1 mM dissolved $FeCl_2$ in the presence of 50 mM CHES, MES,

HEPES, MOPS, and TRIS buffers. Recognizing that it is unlikely precipitation can be avoided with any buffer in Fe-H_2O systems over a significant range of pH, we chose to focus on the environmentally realistic Fe^0-H_2O-CO_2 system. A bicarbonate buffer with total dissolved carbonate = 1.5×10^{-2} *M* was adopted for routine experiments because it provided a reasonable buffer capacity without visible precipitation of iron carbonates during the course of a typical degradation experiment (4-5 hr). This carbonate concentration is also representative of the dissolved CO_2 found in natural groundwaters, typically $\approx 10^{-2}$ *M*.[57]

The development of Eh-pH conditions in our anaerobic Fe^0-H_2O-CO_2 model systems was characterized with needle-form electrodes used during bench-top incubation of serum bottles without added NACs. The Pt electrode potential of the aqueous bicarbonate medium decreased rapidly from about 600 mV (vs. SHE) to <50 mV after 2 hr, followed by a slower gradual decline to around -200 mV after about 6 hr (Figure 2.1). This decrease in measured potential reflects convergence to the equilibrium potential for the Fe^0/Fe^{2+} couple as anaerobic corrosion causes a gradual increase of Fe^{2+} in solution (eq 1-2). The pH of the buffer medium showed a comparatively small increase, about 0.2 units, over 4-5 hr. Therefore, the 2-hr equilibration period prior to initiation of all degradation experiments ensured that they started with relatively stable conditions with respect to Eh and pH.

4.2 Pathway of nitro reduction by Fe^0

The reaction of nitrobenzene by Fe^0 under the conditions of this study produced aniline with nitrosobenzene as an intermediate product. Accounting for these three species gives good mass balance at pH > 5.5 (>85%), but with a reproducible dip at intermediate times (Figure 4.1), which suggests all of the nitrosobenzene formed is not detected in solution and/or that there is an additional reaction intermediate. Phenylhydroxylamine is the most likely intermediate, and may correspond to an unidentified peak with retention time = 1.2 min (cf. ~1.0 min for the solvent peak, 2.2 min for aniline, 3.7 min for nitrobenzene, and 4.2 min for nitrosobenzene). Similar elution patterns have been reported for nitrobenzene reduction in other systems.[43,58] The variation in size of this peak with reaction time suggests an intermediate in reduction from nitrosobenzene to aniline, and similar behavior was observed when nitrosobenzene was used as the initial substrate. However, a standard for phenylhydroxylamine was not

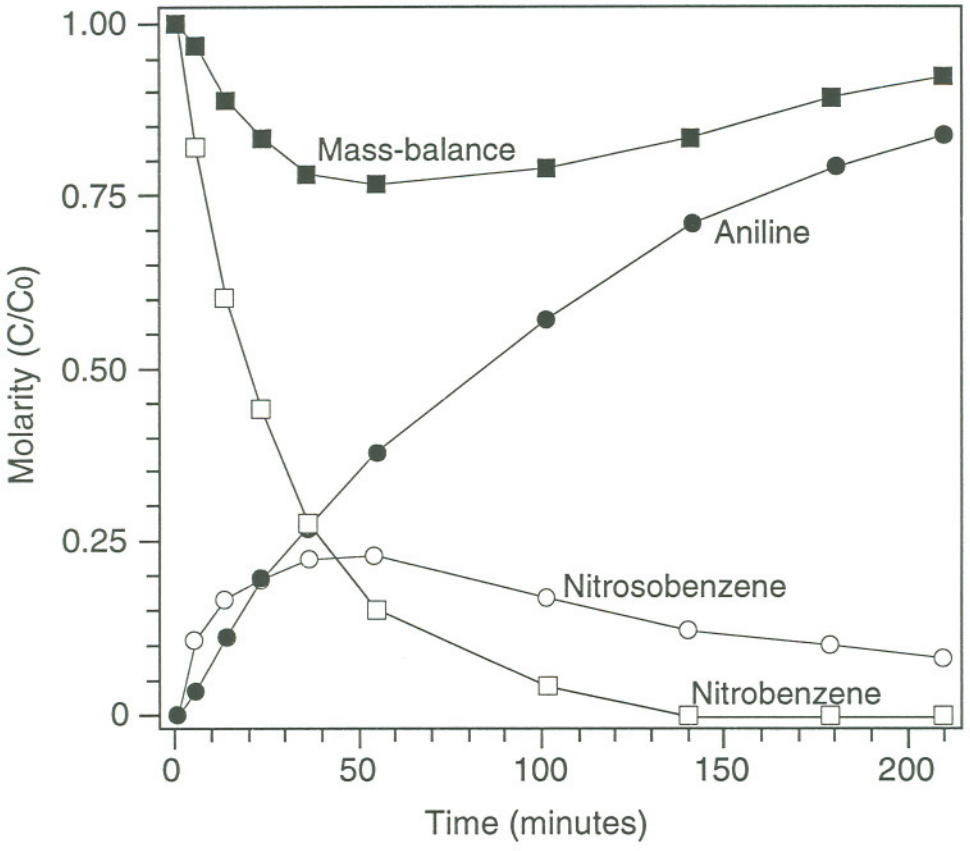

Figure 4.1: Kinetics of nitrobenzene reduction to nitrosobenzene and then to aniline under experimental conditions. 33.3 g/L of 18-20 mesh, acid-washed Fluka iron turnings, preincubated in 1.5 x 10^{-2} *M* bicarbonate buffer (pCO_2 = 0.01 atm) for 2 hr, mixed throughout by rotation at 10 rpm and 15°C. Data are plotted relative to the initial concentration of nitrobenzene (1.5 x 10^{-5} *M*).

available, so this assignment was not confirmed. Neither azoxybenzene or azobenzene were observed as products of nitrobenzene reduction, indicating that condensation reactions (pathways IV-V, Figure 2.2) are insignificant at the substrate concentrations used in this study. The absence of observed azo and azoxy intermediates, suggests that reduction of these compounds (i.e., pathways VI-VII, Figure 2.2) was not a significant contributor to the formation of aniline.

Based on these results, sequential nitro reduction to aniline, via intermediate nitroso and hydroxylamine compounds, appears to be the only important transformation process occurring in the Fe^0-H_2O-CO_2 systems studied. Formally, the overall reaction:

$$Ar\text{-}NO_2 + 3Fe^0 + 4H^+ \rightarrow Ar\text{-}NH_2 + 3Fe^{2+} + 2OH^- \quad (7)$$

occurs in three steps, each involving a 2-electron reduction, with Fe^0 as the ultimate electron donor. The contributing 2-electron reactions can be written:

$$Ar\text{-}NO_2 + Fe^0 + H^+ \xrightarrow{k_1} Ar\text{-}NO + Fe^{2+} + OH^- \quad (8)$$

$$Ar\text{-}NO + Fe^0 + 2H^+ \xrightarrow{k_2} Ar\text{-}NHOH + Fe^{2+} \quad (9)$$

$$Ar\text{-}NHOH + Fe^0 + H^+ \xrightarrow{k_3} Ar\text{-}NH_2 + Fe^{2+} + OH^- \quad (10)$$

where each k represents the observed first-order rate constant for the associated reduction step. The distribution of products depends on the relative values of these rate constants, which, in turn, varies with reaction conditions.

4.3 Kinetics of transformation

Experiments were generally performed with nitrobenzene at an initial concentration of about 1.5×10^{-5} *M*, and the reaction was monitored until >98% complete (~3 hr). Loss of nitrobenzene was found to be <5% over 48 hr in control experiments without Fe^0, so all of the disappearance during the first few hours was attributed to nitro reduction. Natural log concentration versus time plots for nitrobenzene reduction were unambiguously linear over at least 3 half-lives (Figure 4.2), so linear regression of these data was used for routine determination of k_1, the pseudo first-order rate constant for eq

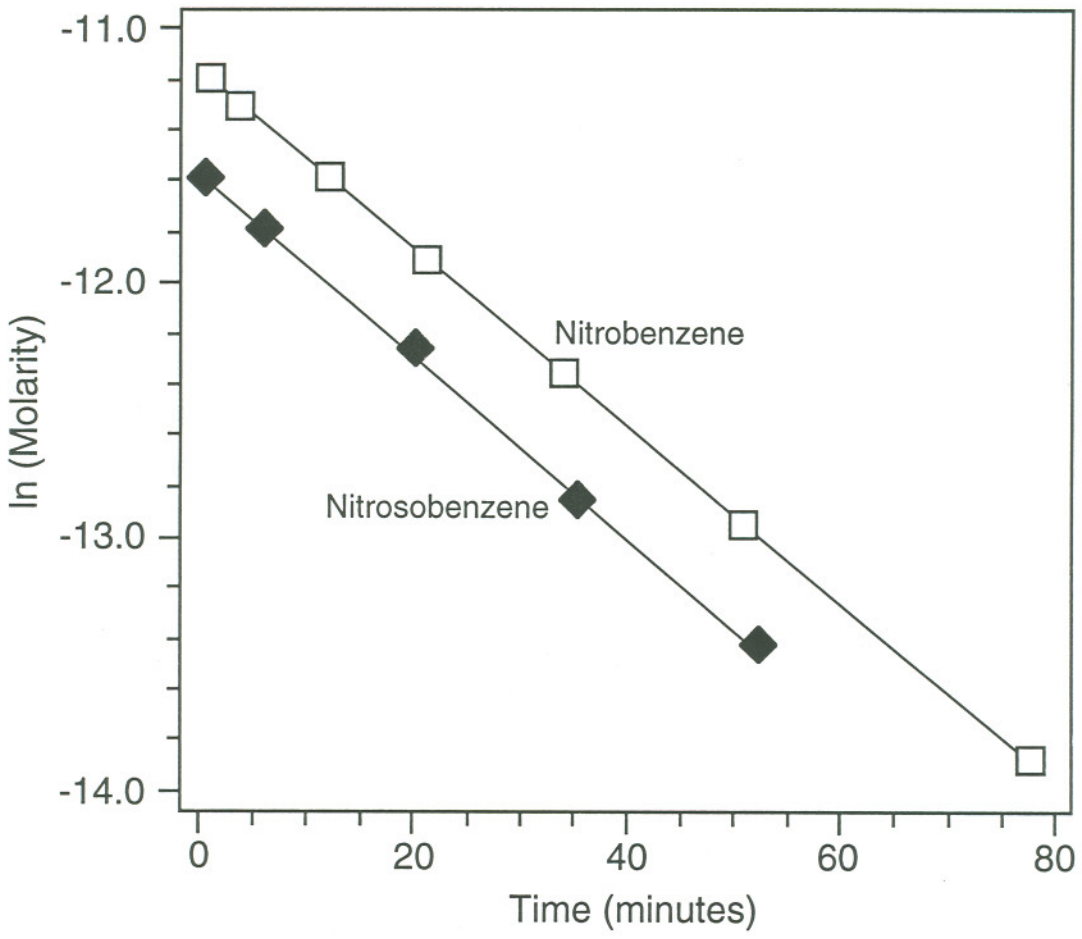

Figure 4.2: Pseudo first-order disappearance of nitrobenzene (same experiment as Figure 4.1) and nitrosobenzene (separate experiment under identical conditions). Linear regression gives reduction rate constants of k_1 = 0.035±0.001 min^{-1} ($t_{1/2}$ = 19.7 min) for nitrobenzene and k_2 = 0.034±0.001 min^{-1} ($t_{1/2}$ = 20.4 min) for nitrosobenzene.

8. As was concluded previously for the dechlorination of CCl_4,[4] the lack of deviation from first-order kinetics indicates that changes in reactivity of the Fe^0 due to corrosion and precipitation are not significant over several hours. However, nitro reduction experiments that were allowed to run to completion did exhibit a small decline in k_1 at exposure times over 1 hr. A similar effect was observed by Gillham and O'Hannesin for the reduction of chlorinated aliphatics in batch experiments.[5]

First-order rate constants for the appearance for nitrosobenzene were obtained by nonlinear regression, assuming a kinetic model for sequential first-order reactions is appropriate.[4,59] For the data in Figure 4.1, the rate constant is 0.069±0.010 min^{-1}, which is roughly twice the value k_1 = 0.035±0.001 min^{-1} obtained by fitting the data for nitrobenzene disappearance. The discrepancy is modest, but appears to be significant, and suggests an additional formation reaction for nitrosobenzene. One such reaction might be the dismutation of phenylhydroxylamine,[60] but no effort was made to test this hypothesis experimentally.

The kinetics of nitrosobenzene reduction (eq 9) were also investigated in two ways. Using nitrosobenzene as the initial substrate, pseudo first-order disappearance was observed, and therefore k_2 could be obtained simply by linear regression of the natural log concentration versus time data. Alternatively, the concentration of nitrosobenzene as an intermediate in nitrobenzene reduction could be fit, by nonlinear regression, to the kinetic model for sequential first-order reactions. For similar conditions, the value of k_2 obtained from nitrobenzene reduction (0.006±0.001 min^{-1}, Figure 4.1) was significantly less than that obtained from nitrosobenzene as the initial substrate (0.034±0.001 min^{-1}, Figure 4.2). This difference may be due to competition for reactive sites on the metal by nitrobenzene and its sequential reduction products. The reduction of phenylhydroxyl-amine (eq 10) was accessible only in terms of aniline appearance. The kinetics of aniline appearance in Figure 4.1 fit a first-order model with a rate constant of 0.009±0.001 min^{-1}.

4.4 Effect of substrate properties.

The similarity in disappearance rates for nitrobenzene and nitrosobenzene (Figure 4.2) suggests a fundamental similarity in the rate controlling processes. However, the diffusion coefficients and the reduction potentials for these two compounds are very similar (Table 2.1), so this result alone can not be used to distinguish diffusion from activation control. Additional experiments were performed with a series of para-

Table 4.1. Effect of substitution on pseudo-first order rate constant of substrate reduction §

Substrate†	D ($cm^2\ s^{-1}$) ¥	$E_{1/2}$ (V) *	k_1 (min^{-1})	$t_{1/2}$ (min)
Nitrosobenzene	7.1×10^{-6}	-0.63[38]	0.0339	20.4
1,3-dinitrobenzene	6.2×10^{-6}	-.25[73]	0.0339	20.4
4-chloronitrobenzene	6.2×10^{-6}	-.40[37]	0.0336	20.6
4-nitroanisole	5.9×10^{-6}	-.55[73]	0.0327	21.2
4-nitrotoluene	6.2×10^{-6}	-0.46[37]	0.0335	20.7
2,4,6-trinitrotoluene	5.6×10^{-6}		0.0330	21.0
Parathion	4.3×10^{-6}	-0.21[77]	0.0250	27.7

§ Conditions: 33.3 g/L acid-washed 18-20 mesh, Fluka granular iron, 1.5×10^{-2} *M* carbonate buffer at pH 5.9, 10 rpm and 15°C.

† Initial NAC concentration = 1.5×10^{-5} *M*.

¥ Molecular diffusivity estimated for aqueous solution at 15°C using method after Tucker and Nelken.[76]

* Polarographic half-wave potentials for aqueous solution at pH 7, references given as superscripts.

substituted nitrobenzenes, selected to exhibit a range of diffusive and electronic properties. The resulting values of k_1 (Table 4.1), show change in nitro reduction rates for substrates with substituents that effect redox potentials without significantly altering diffusion coefficients. The low value of k_1 for parathion corresponds to the significantly decreased diffusion coefficient that results from the bulky p-(O,O-diethyl-phosphorothioate) substituent on the nitrophenyl ring. Of course, the general significance of the implication that mass transfer to the metal limits nitro reduction rates is dependent on the relevance of the conditions under which experiments are performed. For this reason, the following discussion will focus primarily on the effects that medium composition and other experimental design variables have on the observed rate on nitrobenzene reduction.

4.5 Effects of the iron surface

Since the dechlorination of halocarbons by Fe^0 involves reaction at the metal surface,[4,5] it was anticipated that the condition and quantity of metal surface area would also influence the kinetics of nitro reduction. Previous work has shown that treatment of the metal with dilute HCl prior to each experiment accelerates dechlorination rates and improves the reproducibility of reaction rate determinations.[4] In this study, preliminary experiments showed similar effects for nitrobenzene reduction. The greatest increase in k_1 resulted from the combined action of HCl and sonication, so a protocol based on this treatment was adopted for all subsequent experiments. Aside from the practical advantages of increasing the magnitude and reproducibility of the desired reaction rates, our investigations of pretreatment effects also provide insight into the role of the metal surface in contaminant transformation. The observed effect of acid pretreatment may be due to one or more of the following changes: (i) cleaning of the surface by dissolution of metal and breakdown of the passivating oxide layer; (ii) increasing the metal surface area by etching and pitting through corrosion, and formation of large mumber of step-kink sites; (iv) increase in metal surface area due to mechanical abrasion of the during sonication; and (iv) increased concentrations of adsorbed H^+ and Cl^- that persist after pretreatment with HCl.

The effect of acid pretreatment on the physical characteristics of iron surfaces, and the evolution of these characteristics during exposure to aqueous bicarbonate, was studied using scanning electron microscopy (SEM). The grains of Fluka iron turnings are

composed of polycrystalline material with crystal boundaries mostly obscured by a 5-10 mm thick surface coating consisting primarily of iron oxides (Figure 4.3). Acid-treatment of Fe^0 results in complete dissolution of the surface coating, exposure of the crystal boundaries due to preferential etching along these features, and appearance of highly textured crystal surfaces (Figure 4.4). The increased roughness of these surfaces is presumably responsible for the increase in measured specific surface area, from 0.005 m^2/g for the untreated metal to 0.038 m^2/g after acid pretreatment. Corrosion pits were observed, but these features were not abundant, so uniform corrosion appears to have been the predominant mechanism of etching by acid. The sample shown in Figure 4.4 was exposed to carbonate buffer for 1 hr, but no effect of this treatment can be seen due to the short contact time and slow kinetics of siderite precipitation. In contrast, extended exposure of acid-etched Fe^0 to bicarbonate buffer leads to a layer of crystalline precipitate with areas of corrosion along crevices and defects (Figure 4.5). The precipitate layer was shown to consist of siderite ($FeCO_3$) by EDS and X-ray diffraction analysis. Formation of this layer accounts for the decreased specific surface area (from 0.038 to 0.021 m^2/g) measured on an acid-pretreated sample exposed to carbonate buffer for 4 hr. None of the samples studied showed visible evidence of mechanical abrasion due to sonication or mixing by rotation.

Under circumstances where the metal surface condition is effectively constant, the quantity of available surface area is among the most significant experimental variables affecting contaminant reduction rates. Figure 4.6 shows that rate constants for nitrobenzene reduction, k_1, increase linearly with the mass of Fe^0 per unit reaction volume (g/L), over the range of conditions studied. Assuming a constant specific surface area of 0.021 m^2/g, the more general independent variable of surface area concentration, [Surface Area], can be derived. Linear regression on the data for k_1 (min^{-1}) and [Surface Area] (m^2/L) gives

$$k_1 = (0.039 \pm 0.002) \times [\text{Surface Area}] + (0.003 \pm 0.001) \qquad (12)$$

with $r^2 = 0.997$ for $n = 5$, and the uncertainties represent one standard deviation. The resulting intercept appears to be negligible, indicating that nitro reduction by Fe^{2+} is not significant and all disappearance is attributable to reaction with Fe^0. The slope of eq 12 is the specific reaction rate constant; i.e., where k_1 has been normalized to 1 m^2/L of iron.

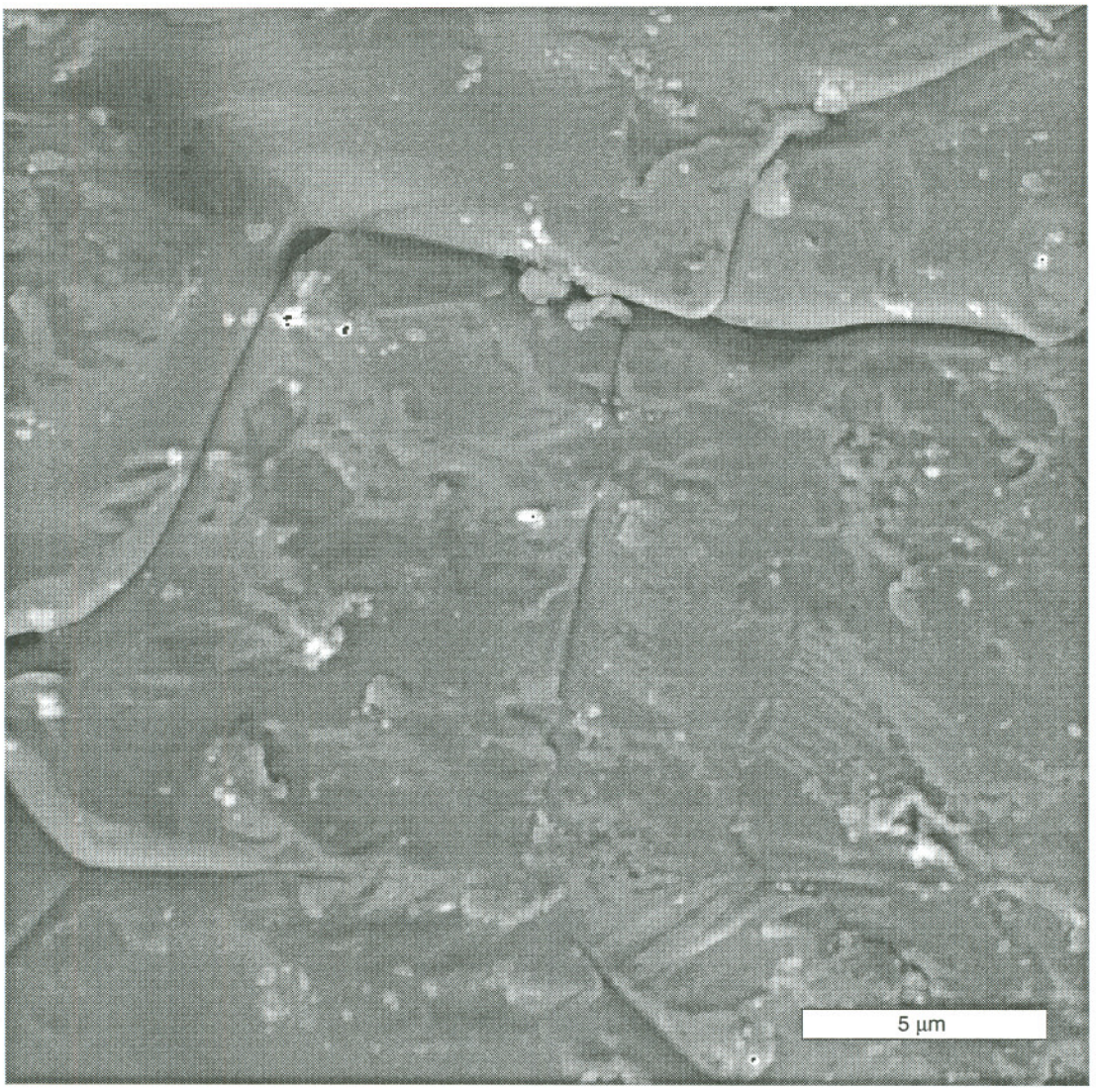

Figure 4.3: Scanning electron micrograph of untreated Fluka iron metal surface, with visible crystal boundaries and oxide film cover; original magnification, x4000.

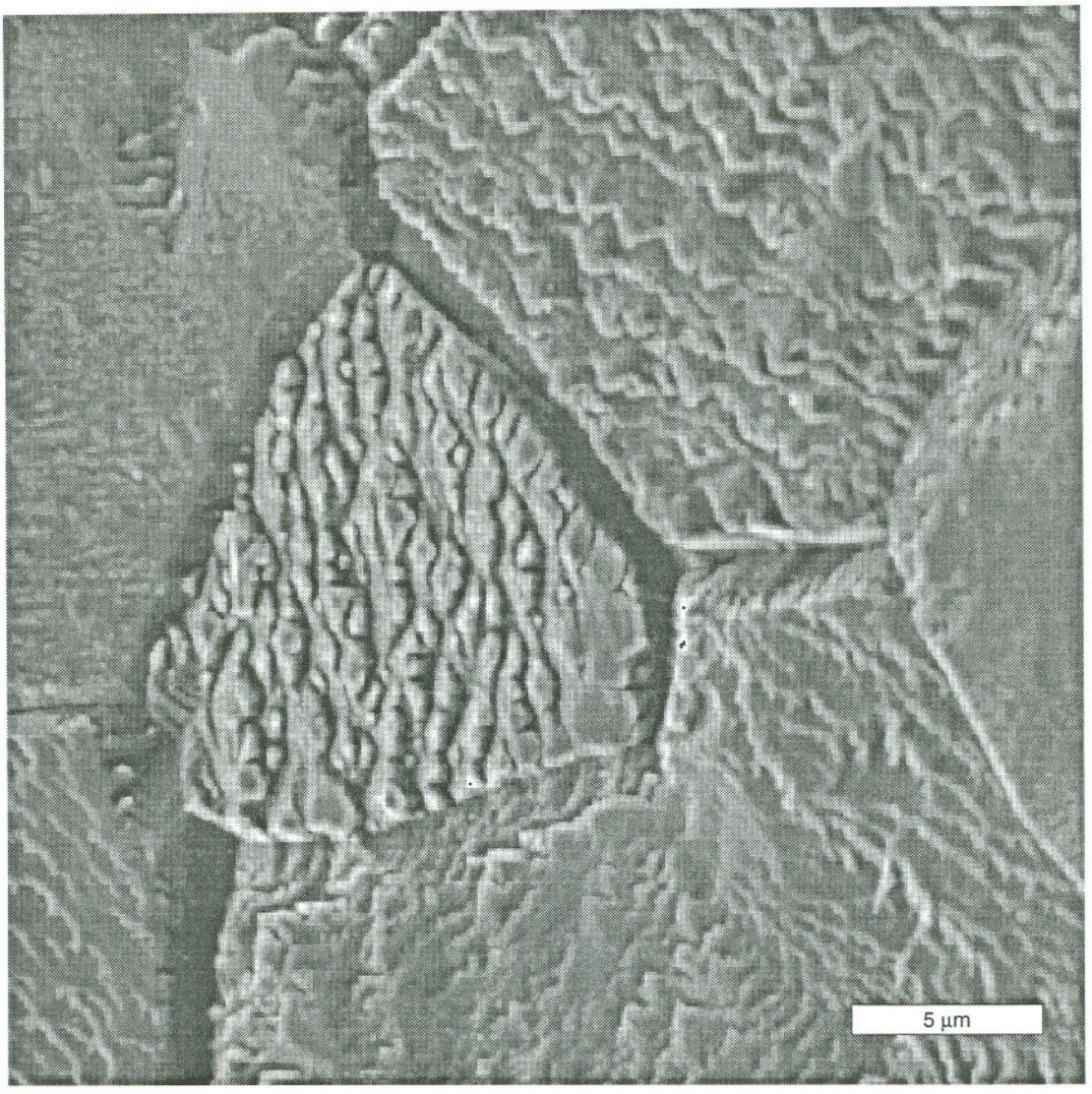

Figure 4.4: Scanning electron micrograph of iron metal surface following treatment in dilute HCl (10% v/v), showing corrosion at crystal boundaries and fine-scale etching of the surface; original magnification: x3000.

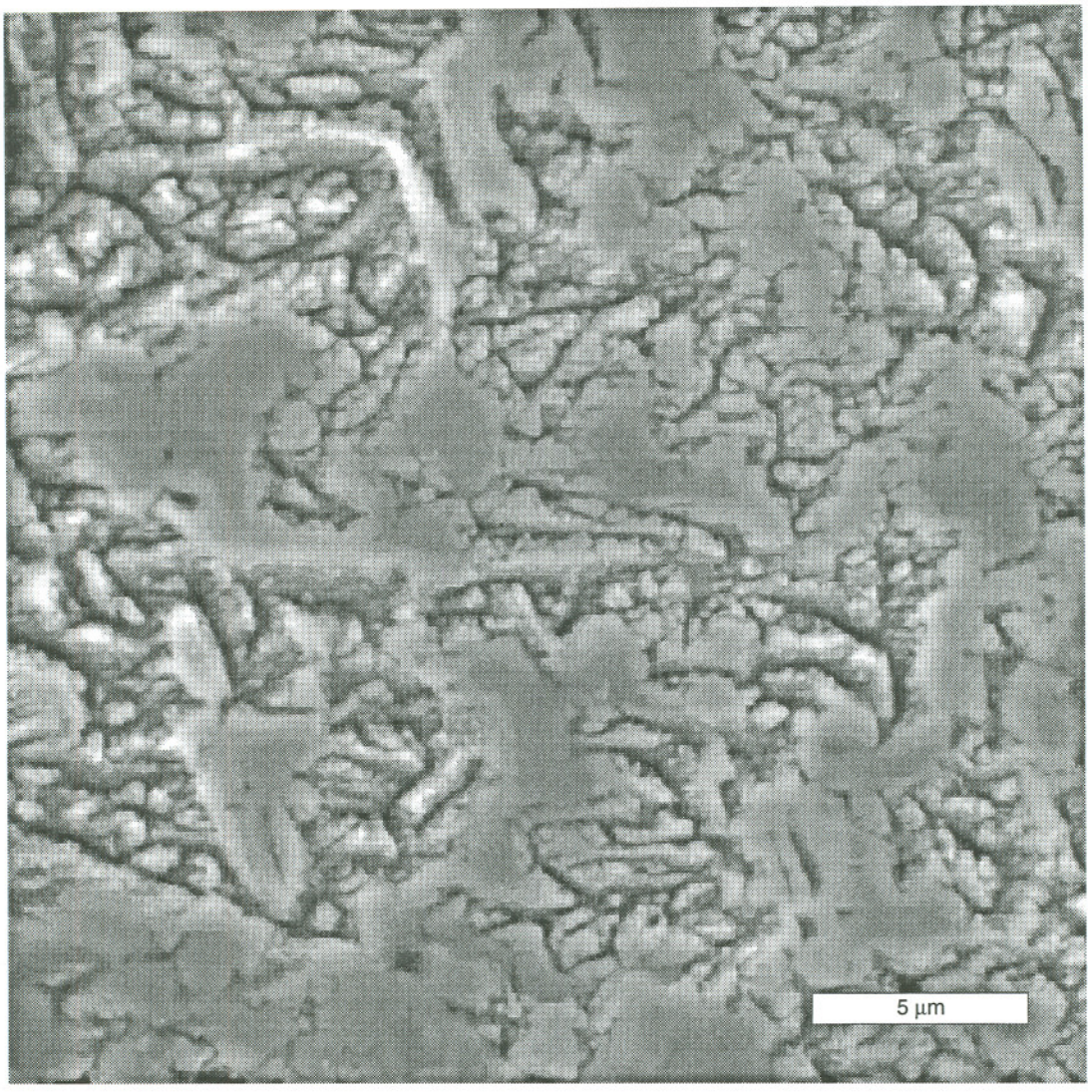

Figure 4.5: Scanning electron micrograph of acid-washed iron, exposed in a bicarbonate buffer (total dissolved carbonate = 0.06 *M*) for 5 days with mixing; original magnification: x3000. It shows accelerated corrosion at crystal boundaries and partial coverage with fine-grained siderite.

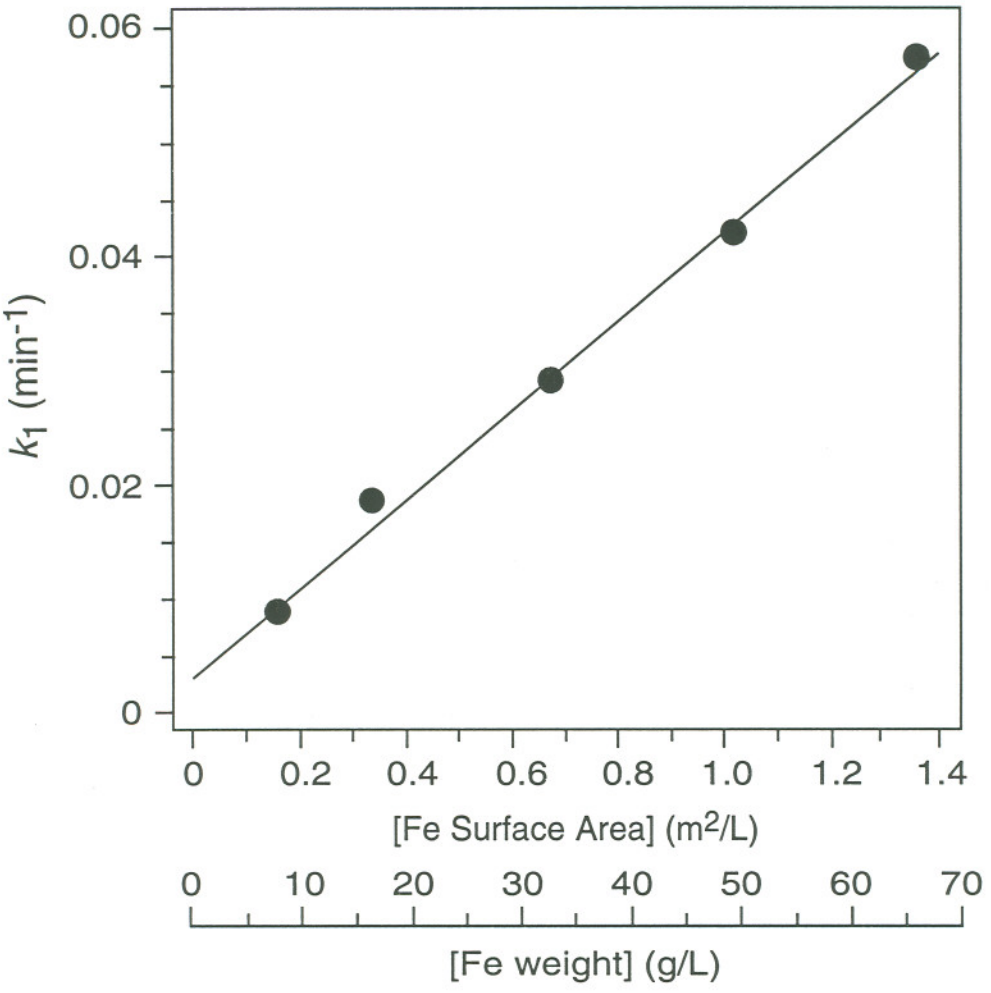

Figure 4.6: Effect of Fe^0 surface area concentration on the pseudo first-order rate constant for nitrobenzene reduction. Experiments were performed by varying mass of 18-20 mesh, acid-washed Fluka iron turnings. All were performed in 1.5 x 10^{-2} *M* bicarbonate buffer at 10 rpm and 15°C, after 2 hr for buffer equilibration. The regression line corresponds to eq 12.

Reduction rates characterized in these terms should be independent of the mass and specific surface area of the metal used and the volume of the reaction system. At present, however, there is no practical way to factor out variation in the density of reactive sites on the metal surface. The latter correction will be particularly important if meaningful comparisons are to be made between iron samples from different sources or with different histories that affect the type and density of surface precipitates. For example, the 16-fold difference between the values $2.5\pm0.2 \times 10^{-3}$ min^{-1} m^{-2} L reported previously for CCl_4 reduction by Fisher iron metal,[4] and $3.9\pm0.2 \times 10^{-2}$ min^{-1} m^{-2} L determined for nitrobenzene in this study probably reflects, in part, differences in the properties of the two organic reactants. However, reactivity per unit surface area of iron is also likely to be a significant variable because the Fe^0 source and pretreatment were not the same in the two studies. The specific reaction rate constants described above offer advantages similar to the half-lives normalized to 1 m^2/mL that have been reported by Gillham and O'Hannesin.[5] One major difference, however, is that the latter are based on single experiments, so they lack the statistical power that derives from regression on a larger quantity of data, as was done to obtain the fitted parameters in eq 12.

4.6 Effect of pH

It was anticipated that changes in pH might cause changes in the nitro reduction rate through (i) direct involvement of H^+ in the contributing reactions (recall eq 8-10), (ii) mass transport limitations imposed by the precipitation of a passive film on the metal surface, and/or (iii) mass transport limitations determined by the thickness of the Nernst layer between the passive film and the bulk electrolyte. Previous studies have shown that decreased pH results in a modest increase in CCl_4 dechlorination rate under conditions that probably were border-line between activation and diffusion control,[4] and a strong increase in dechlorination rate where activation control may have been predominant.[9] In this study, the results indicate no clear effect on k_1 over the environmentally relevant pH range of 6-8, and only a small decrease for pH < 6 (Figure 4.7). Buffer preparation for the two experiments performed at pH < 6 involved addition of HCl, so it is possible that the trend exhibited in Figure 4.7 reflects the influence of Cl^-, a highly corrosive anion, rather than pH. The general lack of a pH effect, however, is consistent with nitro reduction rates that are limited by mass transport to reactive sites on a surface where pH-controlled precipitation reactions are comparatively slow (and ionic strength is roughly constant).

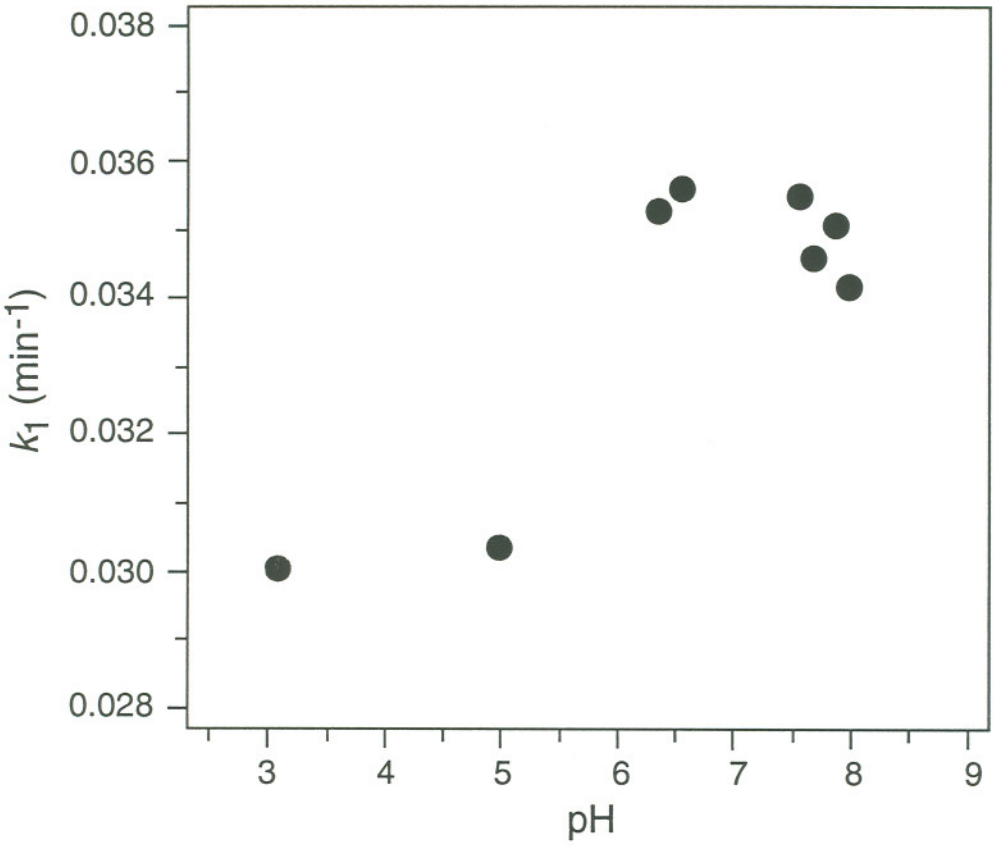

Figure 4.7: Effect of solution pH on the pseudo first-order rate constant for nitrobenzene reduction. All bottles contained 33.3 g/L of 18-20 mesh acid-washed Fluka iron turnings, preincubated in 1.5 x 10^{-2} *M* bicarbonate buffer (pCO_2 = 0.01 atm, initial pH = 5.9) for 2 hr, mixed throughout by rotation at 10 rpm and 15°C.

A more dramatic effect of pH was observed on the distribution of nitro reduction products. Following the disappearance of nitrobenzene and the intermediate nitroso product, the final concentration of aniline provided nearly complete mass balance at pH > 5. Values of k_3, estimated from the rate of aniline appearance, decreased slightly from 0.015 min^{-1} at pH 5 to 0.009 min^{-1} at pH 6.9. However, below pH 5, no aniline production at all was detected. It is unlikely that the lack of aniline appearance at pH < 5 indicates a real change in the product distribution since all of the major transformation pathways produce aniline (Figure 2.2). Instead, protonation of the aniline formed (pK_a = 4.6) probably prevents desorption of the product due to electrostatic attractions involving the anilinium cation and specifically adsorbing counter-ions such as Cl^-.[61]

4.7 Effect of bicarbonate

In most natural waters, ambient levels of pCO_2 and alkalinity determine the pH and carbonate speciation. In the presence of Fe^0, H_2CO_3 and HCO_3^- can be reduced, and thereby accelerate corrosion (eqs 5-6), or precipitate as siderite, which eventually will inhibit corrosion by limiting mass transfer to the metal surface. The net impact of these phenomena on the application of Fe^0 to remediation of contaminated groundwaters can be predicted from results obtained in this study using CO_2-buffered model systems. In early experiments, it was observed that k_1 was notably greater in the presence of moderate concentrations of carbonate buffer, relative to unbuffered systems at comparable pH. This increase in k_1 appears to be due to carbonate-enhanced corrosion in the absence of significant precipitation. In subsequent experiments, it was discovered that k_1 decreased at high total carbonate concentrations (Figure 4.8) and with extended exposure to a particular bicarbonate buffer (Figure 4.9; Table 4.2). Thus, nitro reduction rates decline as circumstances that favor precipitation of iron carbonates improve. This is consistent with the observation that a gray solid (presumably siderite) formed in serum bottles that were left unopened for several days after the reduction experiment, and with reports in the literature that the kinetics of siderite precipitation are relatively slow.[34,35] SEM of iron samples after varying degrees of exposure to aqueous carbonate confirms this interpretation: little authigenic material was evident after 2 hr, but 5 days of exposure produced a dense film of precipitate (Figure 4.5). It was confirmed by EDS and XRD that the precipitate film consisted almost exclusively of siderite. Precipitates such as siderite that are not redox active, or are much less redox active than the underlying zero-valent metal, generally will inhibit contaminant reduction by creating a barrier for mass

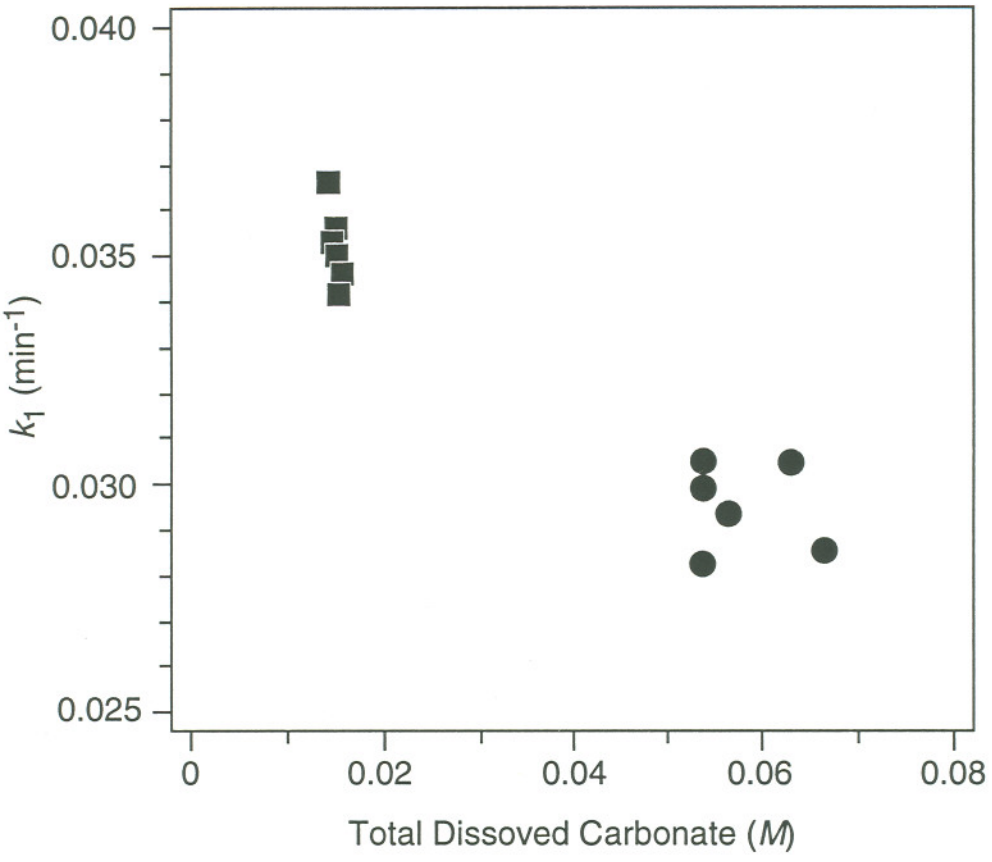

Figure 4.8: Effect of total dissolved carbonate concentration on the pseudo first-order rate constant for nitrobenzene reduction. Total carbonate of buffer medium was ~1.5 x 10^{-2} and 6.0 x 10^{-2} *M*, respectively. All bottles contained 33.3 g/L of 18-20 mesh acid-washed Fluka iron turnings, preincubated for 2 hr, mixed throughout by rotation at 10 rpm and 15°C.

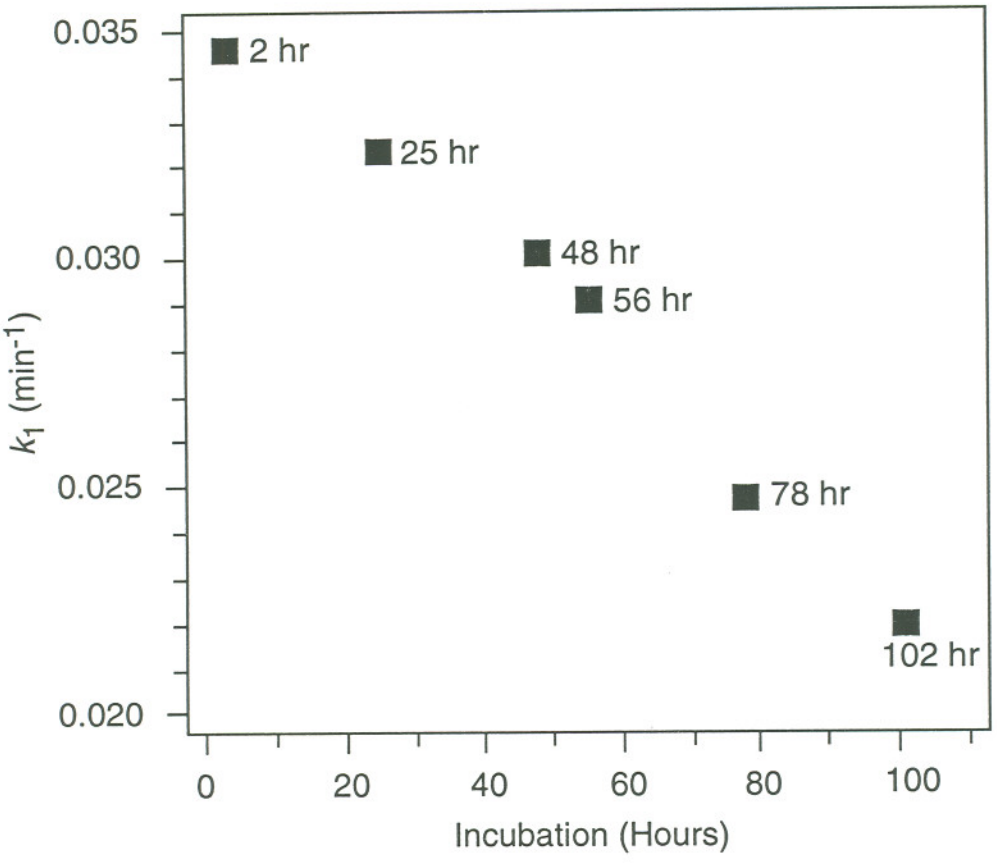

Figure 4.9: Effect of extended incubation of Fluka Fe^0 with bicarbonate buffer on pseudo first-order rate constants for nitrobenzene reduction. Bottles containing 33.3 g/L of 18-20 mesh acid-washed Fluka iron turnings, were preincubated variable amounts of time in 1.5 x 10^{-2} *M* bicarbonate buffer (pCO_2 = 0.01 atm, initial pH = 5.9), with mixing throughout by rotation at 10 rpm and 15°C. Figure 2.1 and Table 4.2 show the trend of measured Eh and pH during this experiment.

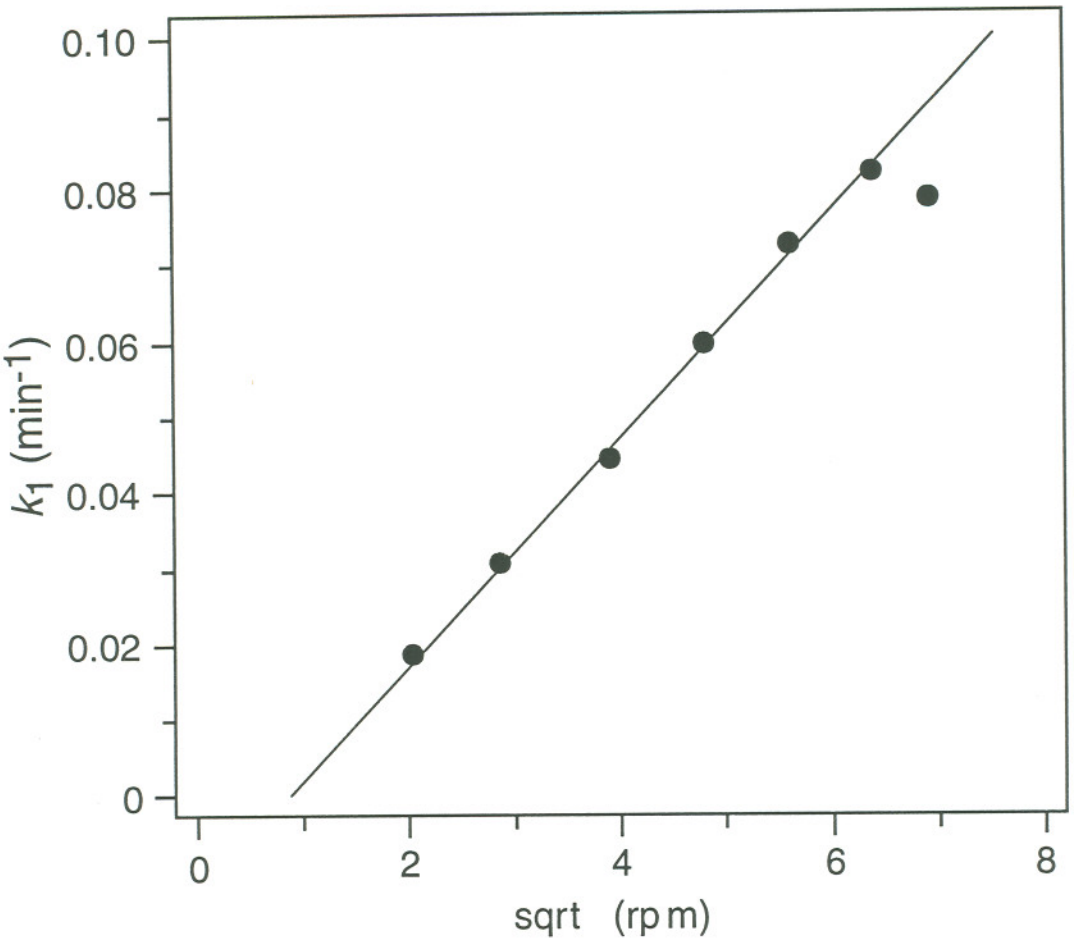

Figure 4.10: Effect of mixing rate on the pseudo first-order rate constant for nitro-benzene reduction. All bottles contained 33.3 g/L of 18-20 mesh acid-washed Fluka iron turnings, preincubated in 1.5 x 10^{-2} *M* bicarbonate buffer (pCO_2 = 0.01 atm, initial pH = 7.9) for 2 hr, mixed throughout by rotation at 15°C.

Table 4.2: Effect of extended exposure of Fe^0 in bicarbonate medium on pseudo-first order rate constant of nitrobenzene reduction §

Exposure Time (hr)†	E (mV vs SHE)¥	pH Condition*	k_1 (min^{-1})	$t_{1/2}$ (min)
2	55	5.87	0.0347	20.0
25	-152	6.57	0.0328	21.1
48	-248	6.52	0.0304	22.8
55	-298	6.37	0.0293	23.7
80	-321	6.16	0.0251	27.6
102	-332	6.12	0.0237	29.2

§ Conditions: 33.3 g/L acid-washed 18-20 mesh Fluka granular iron, 1.5×10^{-2} *M* bicarbonate buffer, initial nitrobenzene concentration = 1.5×10^{-5} *M*, 10 rpm and 15°C.

† Exposure time in bicarbonate buffer.

¥ Final measured Eh values.

* Final measured pH values.

transport to active sites. Defects such as the cracks shown in Figure 4.5 prevent the passive film from being fully protective with respect to corrosion of the metal, which in turn allows for sustained reduction at the metal surface. Therefore, these features may prove to be important determinants of field performance in contaminant remediation.

4.8 Effect of mixing rate

The usual method of mixing employed in this study was 360° rotation at 10 rpm around a fixed-length axis. Since the rate of rotation was rapid relative to the rate of reaction, rpm should be linearly related to the actual velocity of mixing experienced by the metal (at least, until centrifugal forces become significant). Numerous empirical determinations have shown that this velocity is proportional to the square of the mass-transfer coefficient for diffusion across a stagnant boundary layer.[62] Therefore, nitro reduction rate constants should exhibit a linear relationship with respect to $(rpm)^{0.5}$, under conditions where the reaction is mass transport limited. Values of k_1 measured in this study increased linearly with $(rpm)^{0.5}$ up to about 45 rpm (Figure 4.10) and regression on these data gives

$$k_1 = (0.015 \pm 0.001) \times (rpm)^{1/2} - (0.015 \pm 0.002) \qquad (13)$$

where $r^2 = 0.998$ for $n = 6$, and the uncertainties represent one standard deviation. The result provides further evidence for the conclusion that nitro reduction rates are mass transport limited under the conditions of this study. Again, comparison with the previously reported study of CCl_4 dechlorination,[4] shows that the systems behave similarly.

4.9 Mechanism of nitro reduction

Since nitro reduction is a surface reaction between the organic reactant and the metal, it must progress through the following steps: (i) mass-transfer and adsorption of the reactant to the solid surface, (ii) chemical reaction at the surface, and (iii) desorption and mass-transfer away from surface. The data indicated that, under the conditions of this study, mass transport of NACs to the iron surface is rate-limiting and determines the observed first-order rate of disappearance. Competition between desorption and further reduction determines the degree to which intermediate transformation products are

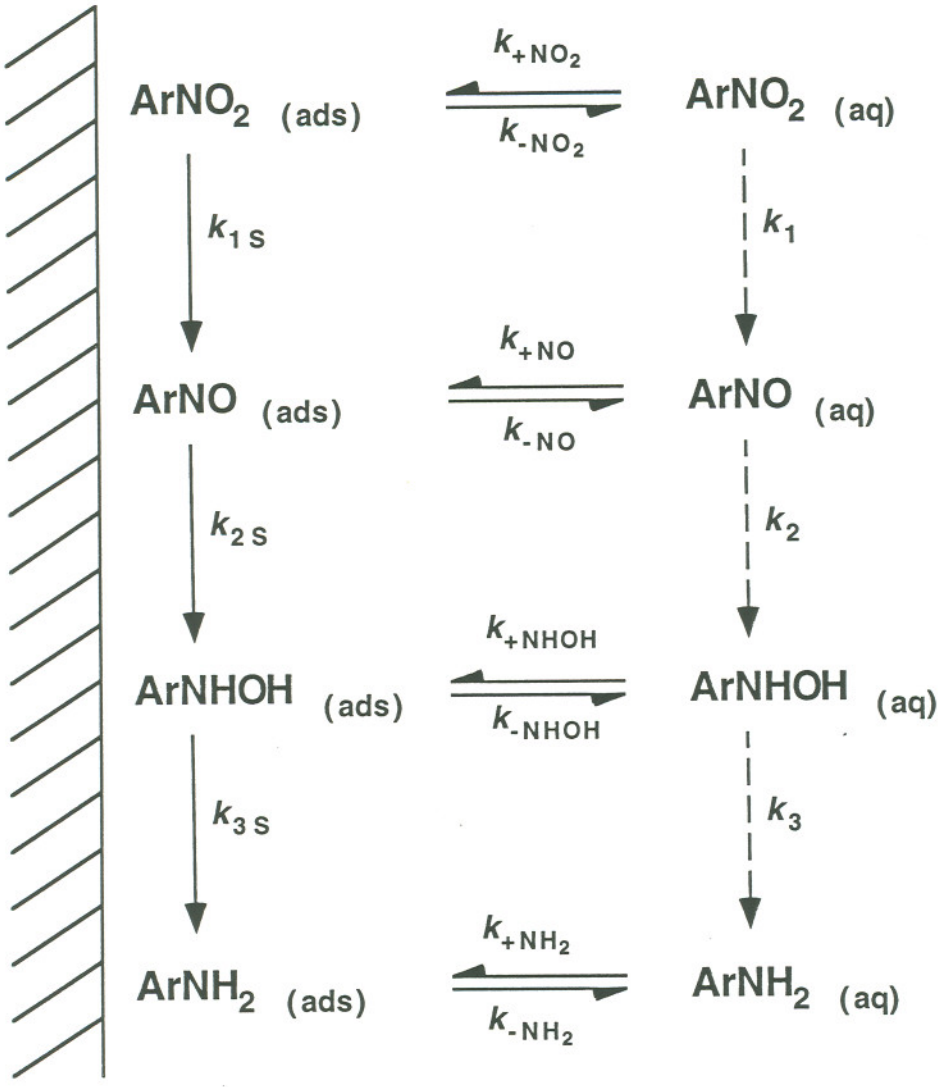

Figure 4.11: Scheme showing competing sequences of substrate adsorption and reduction at a metal surface. The dashed arrows represent the transformation process that was observed by analysis of the solution phase, but reaction took place primarily through adsorption and reduction at the surface (represented by solid arrows).

observed in the solution. This relationship is illustrated in Figure 4.11 for reduction of nitrobenzene. Appearance of nitrosobenzene as an intermediate in this study implies that its desorption is rapid relative to further reduction to the hydroxylamine (i.e., the step corresponding to k_{-NO} is rapid in comparison to that corresponding to k_{2S}). It is important to note that $ArNHOH_{(ads)}$ must still be formed even though $ArNHOH_{(aq)}$ was not identified, just as $ArNO_{(ads)}$ is believed to be an intermediate in electrochemical nitro reduction even though $ArNO_{(aq)}$ is rarely detected.[43,63] An analogous situation probably exists with dechlorination reactions caused by iron metal. In this case, sequential dechlorination is likely to be the dominant reduction pathway at the metal surface,[4] even though the distribution of products in solution generally does not show the appropriate amounts of intermediate species. The major reason for this is, again, that the distribution of products observed in the aqueous phase is determined by the rates at which various species undergo desorption and transport away from the metal as well as the intrinsic rates of the reductive dechlorination at the surface.

To be more precise about the mechanism of nitro reduction, it is necessary to clarify the nature of the interface where reduction is occurring (represented by the vertical line in Figure 4.11). The thin film of corrosion products that inevitably forms on iron between the bulk metal and aqueous solution consists initially of $Fe(OH)_2$ under anaerobic conditions, but eventually develops a complex layered structure as the result of recrystallization, oxidation, and further precipitation.[64] The presence of carbonate adds further complexity to this surface film through the precipitation of $FeCO_3$. The surface film will contain a population of Fe^{2+} sites as long as reduction by the underlying Fe^0 is competitive with oxidation to Fe^{2+}.[65] Recently, it has been shown that Fe^{2+} adsorbed to a variety of metal oxides is effective at reducing NACs.[66,67] Considering all of the above, it is apparent that nitro reduction may occur (i) at the interface between the electrolyte and surface film, (ii) within the surface film, (iii) at the interface between the surface film and bulk metal, or (iv) at the interface between electrolyte and the bulk metal where the surface film is discontinuous. The latter mechanism will almost certainly offer the highest specific reduction rate, but the degree to which bare metal reaction sites are available in our model systems is uncertain and they are likely to be less common under field conditions. Recent studies on the reduction of O_2 at rust covered iron electrodes (formally equivalent to eq 3) have concluded that this reaction occurs within the oxide film on the metal surface.[65] Presumably, the zone of reduction where Fe^{2+} becomes available will shift outward to the oxide film-electrolyte interface under conditions where oxidants in

the bulk solution are relatively scarce, such as they will be in most applications of iron metal to remediating groundwater. In addition, the ability of nitrobenzene to diffuse into the oxide film is presumably less than that of oxygen. Therefore, it seems that a significant portion of nitro reduction that occurs under environmental conditions is likely to take place at the ferrous oxide-electrolyte interface.

After transport to the interface, and prior to the chemical reduction step, the NAC must form a surface complex. For nitrobenzene this may involve (i) an electron donor-acceptor interaction between d-orbitals of the metal and the p-electron cloud of the aromatic ring lying planar to the surface or (ii) an edgewise interaction, either through the ring hydrogens, or the oxygens of the nitro group.[56,68] Not surprisingly, the strength and orientation of NAC-surface interaction is strongly affected by environmental factors such as the presence of specifically adsorbing counter-ions. The range of possible surface complexes may result in significant differences in the surface reaction rate. For example, electrochemical studies have shown that the planar interaction will favor electron transfer to the NAC, whereas an edgewise interaction with the nitro group pointing away from the surface is more favorable for protonation of the resulting anion radical.[69] Similar distinctions can be formulated for all the sequential products of nitro reduction. Aniline can not be further reduced by iron, and, in fact, is a well-known corrosion inhibitor. The mechanism of inhibition is believed to be simple interference with mass transport of oxidant to the metal surface, which, in turn, is strongly influenced by the orientation of aniline adsorption.[61] Corrosion inhibition by this mechanism implies that contaminant reduction rates may also be limited by competition for reactive sites on the metal. This would be consistent with the kinetics of nitrosobenzene reduction observed in this study (Figures 4.1-4.2), and may have general significance to the application of Fe^0 as a reducing agent in groundwater remediation.

A likely reduction mechanism for the adsorbed NAC involves the planar donor-acceptor complex as a precursor to electron transfer.[42,69] The adsorbed molecule must undergo a series of electron transfers, proton transfers, and dehydrations to achieve complete reduction, and the order of these steps has been the subject of many detailed electrochemical studies. For example, nitro reduction may be initiated by electron transfer to form an anion radical,[63,70] or protonation to form a cation which then accepts an electron.[71] The precise sequence will vary as a function of pH, solvent properties, and composition of the surface where adsorption and reaction occur. Schwarzenbach et al.[58,66,72] have concluded that electron transfer is initiating and rate limiting in several

homogeneous model systems based on correlations of nitro reduction rates to one-electron reduction potentials. In this study, reduction rates reflect mass transport to the metal surface, so there is no correlation to the energetics of electron transfer. Mass transport also influences the kinetics of further degradation, and therefore the distribution of detectable reduction products. Therefore, the sequence of electron and proton transfer is unlikely to have a discernible effect on the reaction of NACs by Fe^0 under environmental conditions where the metal surface develops a passivating diffusion boundary of iron oxides or carbonates.

Chapter 5

Conclusions

It has long been known that iron metal reduces NACs, but a detailed study of the reaction kinetics, and how the kinetics determine product distributions, has not been reported previously. Electrochemical nitro reduction has been studied extensively, but the results differ significantly from those obtained in this study, for conditions designed to be relevant to groundwater remediation. As expected, nitro reduction occurs rapidly with the corresponding amine as the primary product. However, the major intermediate detected in the aqueous phase was the nitroso compound and not the more commonly observed hydroxylamine. At pH < 5.0, only nitrosobenzene was observed in the aqueous phase. These results have been interpreted in terms of a sequential reduction process from nitro to nitroso, and then to amine via the hydroxylamine. The chemical reduction steps are fast in comparison with mass transfer to the surface, so product distributions are determined by diffusion-limited adsorption/desorption rates of the reacting organics.

Deposition of non-reactive precipitates adds to the diffusion barrier which limits the rate of contaminant reduction that can be achieved. This was shown with siderite ($FeCO_3$), which forms on granular iron in batch model systems at dissolved carbonate concentrations typical of natural groundwaters ($\approx 10^{-2}$ *M*). Rates of nitro reduction decrease with increased concentration of carbonate buffer and increased exposure time to a particular buffer, due to the precipitation of $FeCO_3$. As expected, other experimental conditions that increase substrate access to the metal surface also accelerate nitro reduction (such as rapid mixing and cleaning or etching the metal) whereas very little effect was observed from changes in substrate reduction potential (e.g., by varying substituents).

This study has several implications for the application of iron metal to remediation of contaminated groundwater. First, the rapid nitro reduction by iron may be of direct use in treatment of waters contaminated with NACs, if the resulting amines can be removed by subsequent treatment. In comparison with dechlorination, nitro reduction

is significantly faster, but the products of reduction are of greater environmental concern. Second, the precipitation of iron carbonate on metal surfaces in the subsurface will have a detrimental effect on remediation performance although it appears that contaminant reduction continues even in the presence of substantial precipitation of this solid. In general, it will be the case with all contaminants, that maximizing access to clean metal surfaces will achieve the most rapid and complete degradation.

References

(1) O'Hannesin, S. F. A Field Demonstration of a Permeable Reaction Wall for the In Situ Abiotic Degradation of Halogenated Aliphatic Organic Compounds. M.S. Thesis, University of Waterloo, Ontario, 1993.

(2) *Extended Abstracts of the Symposium on Contaminant Remediation with Zero-Valent Metals; 209th National Meeting,* Anaheim, CA, American Chemical Society, 1995; Vol. 35, No. 1, pp. 691-835.

(3) Gillham, R. W.; Blowes, D. W.; Ptacek, C. J.; O'Hannesin, S. Use of zero-valent metals for in situ remediation of contaminated ground water. In *Proceedings of the 33rd Hanford Symposium on Health & the Environment—In Situ Remediation: Scientific Basis for Current and Future Technologies,* Pasco, WA, Battelle Pacific Northwest Laboratories, 1994; Vol. 2, pp. 913-930.

(4) Matheson, L. J.; Tratnyek, P. G. Reductive dehalogenation of chlorinated methanes by iron metal. *Environ. Sci. Technol.* **1994**, *28*, 2045-2053.

(5) Gillham, R. W.; O'Hannesin, S. F. Enhanced degradation of halogenated aliphatics by zero-valent iron. *Ground Water* **1994**, *32*, 958-967.

(6) Johnson, T. L.; Tratnyek, P. G. A column study of carbon tetrachloride dehalogenation by iron metal. In *Proceedings of the 33rd Hanford Symposium on Health & the Environment—In Situ Remediation: Scientific Basis for Current and Future Technologies,* Pasco, WA, Battelle Pacific Northwest Laboratories, 1994; Vol. 2, pp. 931-947.

(7) Schreier, C. G.; Reinhard, M. Transformation of chlorinated organic compounds by iron and manganese powders in buffered water and in landfill leachate. *Chemosphere* **1994**, *29*, 1743-1753.

(8) Lipczynska-Kochany, E.; Harms, S.; Milburn, R.; Sprah, G.; Nadarajah, N. Degradation of carbon tetrachloride in the presence of iron and sulphur containing compounds. *Chemosphere* **1994**, *29*, 1477-1489.

(9) Warren, K. D.; Arnold, R. G.; Bishop, T. L.; Lindholm, L. C.; Betterton, E. A. Kinetics and mechanism of reductive dehalogenation of carbon tetrachloride using zero-valence metals. *J. Haz. Mater.* **1995**, in press.

(10) Hartter, D. R. The use and importance of nitroaromatic chemicals in the chemical industry. In *Toxicity of Nitroaromatic Compounds*; Rickert, D. E., Ed.; Hemisphere: Washington, DC, 1985; pp. 1-13.

(11) Kagan, J.; Wang, T. P.; Benight, A. S.; Tuveson, R. W.; Wang, G.-R. The phototoxicity of nitro polycyclic aromatic hydrocarbons of environmental importance. *Chemosphere* **1990**, *20*, 453-466.

(12) Leuenberger, C.; Czuczwa, J.; Tremp, J.; Giger, W. Nitrated phenols in rain: Atmospheric occurrence of phytotoxic pollutants. *Chemosphere* **1988**, *17*, 511-515.

(13) Spanggord, R. J.; Mabey, W. R.; Chou, T. W.; Smith, J. H. Environmental fate of selected nitroaromatic compounds in the aquatic environment. In *Toxicity of Nitroaromatic Compounds*; Rickert, D. E., Ed.; Hemisphere: Washington, DC, 1985; pp. 15-33.

(14) Dickel, O.; Haug, W.; Knackmuss, H.-J. Biodegradation of nitrobenzene by a sequential anaerobic-aerobic process. *Biodegradation* **1993**, *4*, 187-194.

(15) Bollag, J.-M. Decontaminating soil with enzymes. *Environ. Sci. Technol.* **1992**, *26*, 1876-1881.

(16) Archer, W. L.; Simpson, E. L. Chemical profile of polychloroethanes and polychloroalkenes. *Ind. Eng. Chem. Prod. Res. Dev.* **1977**, *16*, 158-162.

(17) Silverman, D. D.; Puyear, R. B. Effects of environmental variables on aqueous corrosion. In *Metals Handbook*; 9th ed.; Korb, L. J.; Olson, D. L., Eds.; ASM: Metals Park, OH, 1987; Vol. 13; pp. 37-44.

(18) Shoesmith, D. W. Kinetics of aqueous corrosion. In *Metals Handbook*; 9th ed.; Korb, L. J.; Olson, D. L., Eds.; ASM: Metals Park, OH, 1987; Vol. 13; pp. 45-49.

(19) Pou, T. E.; Murphy, O. J.; Young, V.; Bockris, J. O. M. Passive films on iron: the mechanism of breakdown in chloride containing solutions. *J. Electrochem. Soc.* **1984**, *131*, 1243-1251.

(20) Sato, N. An overview of the passivity of metals. *Corr. Sci.* **1990**, *31*, 1-19.

(21) Salvarezza, R. C.; Videla, H. A.; Arvia, A. J. The electrodissolution and passivation of mild steel in alkaline sulphide solutions. *Corr. Sci.* **1982**, *22*, 815-829.

(22) Sato, N. The stability of pitting dissolution of metals in aqueous solution. *J. Electrochem. Soc.* **1982**, *129*, 260-264.

(23) Bockris, J. O. M.; Khan, S. U. M. *Surface Electrochemistry. A Molecular Level Approach*; Plenum: New York, 1993.

(24) Keddam, M.; Oltra, R.; Colson, J. C.; Desestret, A. Depassivation of iron by straining and by abrasion: An A.C. impedance study. *Corr. Sci.* **1983**, *23*, 441-445.

(25) *Advances in CO_2 Corrosion. Vol 1. Proceedings of the Corrosion/83 Symposium on CO_2 Corrosion in the Oil and Gas Industry*; Hausler, R. H.; Godard, H. P., Eds.; National Association of Corrosion Engineers: Houston, TX, 1984.

(26) Schmitt, G. Fundamental aspects of CO_2 corrosion. In *Advances in CO_2 Corrosion. Vol 1. Proceedings of the Corrosion/83 Symposium on CO_2 Corrosion in the Oil and Gas Industry*; Hausler, R. H.; Godard, H. P., Eds.; National Association of Corrosion Engineers: Houston, TX, 1984; pp. 10-19.

(27) Turgoose, S.; Cottis, R. A.; Lawson, K. Modeling of electrode processes and surface chemistry in carbon dioxide containing solutions. In *Computer Modeling in Corrosion*; Munn, R. S., Ed.; American Society for Testing and Materials: Philadelphia, 1992; Vol. ASTM STP 1154; pp. 67-81.

(28) Wieckowski, A.; Ghali, E.; Szlarczyk, M.; Sobkowski, J. The behaviour of iron electrode in CO_2-saturated neutral electrolyte—I. Electrochemical study. *Electrochim. Acta* **1983**, *28*, 1619-1626.

(29) Wieckowski, A.; Ghali, E.; Szlarczyk, M.; Sobkowski, J. The behaviour of iron electrode in CO_2-saturated neutral electrolyte—II. Radiotracer study and corrosion considerations. *Electrochim. Acta* **1983**, *28*, 1627-1633.

(30) Azuma, M.; Hashimoto, K.; Hiramoto, M.; Watanabe, M.; Sakata, T. Electrochemical reduction of carbon dioxide on various metal electrodes in low-temperature aqueous $KHCO_3$ media. *J. Electrochem. Soc.* **1990**, *137*, 1772-1778.

(31) Hardy, L. I. Formation of Hydrocarbons from the Reduction of Aqueous CO_2 by Zero-Valent Iron. M.S. Thesis, University of Waterloo, Ontario, 1994.

(32) Pourbaix, M. *Atlas of Electrochemical Equilibria in Aqueous Solutions*; Pergamon: Oxford, 1966.

(33) Bruno, J.; Wersin, P.; Stumm, W. On the influence of carbonate in mineral dissolution: II. The solubility of $FeCO_3$ (s) at 25°C and 1 atm total pressure. *Geochim. Cosmochim. Acta* **1992**, *36*, 1149-1155.

(34) Wajon, J. E.; Goen-Eng, H.; Murphy, P. J. Rate of precipitation and formation of mixed iron-calcium carbonates by naturally occurring carbonate materials. *Wat. Res.* **1985**, *19*, 831-837.

(35) Greenberg, J.; Tomson, M. Precipitation and dissolution kinetics and equilibria of aqueous ferrous carbonate vs temperature. *Appl. Geochem.* **1992**, *7*, 185-190.

(36) Fry, A. J. Electrochemistry of nitro compounds. In *The Chemistry of Amino, Nitroso, and Nitro Compounds and their Derivatives*; Patai, S., Ed; Wiley-Interscience: Chichester, 1982; Vol. 1; pp. 319-337.

(37) Kemula, W.; Krygowski, T. M. Nitro compounds. In *Encyclopedia of Electrochemistry of the Elements*; Bard, A. J.; Lund, H., Eds.; Marcel Dekker: New York, 1979; Vol. 13; pp. 77-130.

(38) Kemula, W.; Krygowski, T. M. Nitroso compounds. In *Encyclopedia of Electrochemistry of the Elements*; Bard, A. J.; Lund, H., Eds.; Marcel Dekker: New York, 1979; Vol. 13; pp. 131-161.

(39) Zuman, P.; Shah, B. Addition, reduction, and oxidation reactions of nitrosobenzene. *Chem. Rev.* **1994**, *94*, 1621-1641.

(40) Lund, H. Cathodic reduction of nitro compounds. In *Organic Electrochemistry*; Baizer, M. M., Ed; Marcel Dekker: New York, 1973; pp. 315-345.

(41) Thomas, F. G.; Boto, K. G. The electrochemistry of azoxy, azo and hydrazo compounds. In *The Chemistry of the Hydrazo, Azo and Azoxy Groups*; Patai, S., Ed.; Wiley: New York, 1975; pp. 443-474.

(42) Holleck, L.; Kastening, B. Über den mechanismus der polarographischen reduktion aromatischer nitroverbindungen. *Rev. Polarogr.* **1963**, *11*, 129-140.

(43) Shindo, H.; Nishihara, C. Detection of nitrosobenzene as an intermediate in the electrochemical reduction of nitrobenzene on Ag in a flow reactor. *J. Electroanal. Chem.* **1989**, *263*, 415-420.

(44) Martigny, P.; Simonet, J. On the existence of the intermediate nitroso during the mixed electrochemical reduction of nitro compounds and organic halides. *J. Electoanal. Chem.* **1983**, *148*, 51-60.

(45) Pizzolatti, M. G.; Yunes, R. A. Azoxybenzene formation from nitrosobenzene and phenylhydroxylamine. A unified view of the catalysis and mechanisms of the reactions. *J. Chem. Soc. Perkin Trans.* **1990**, *2*, 759-764.

(46) Dalmagro, J.; Yunes, R. A.; Simionatto, E. L. Mechanism of reaction of azobenzene formation from aniline and nitrosobenzene in basic conditions, general base catalysis by hydroxide ion. *J. Phys. Org. Chem.* **1994**, *7*, 399-402.

(47) Laviron, E.; Vallat, A. Thin layer linear sweep voltammetry. A study of the condensation of nitrosobenzene with phenylhydroxylamine. *Electroanal. Chem. Interfac. Electrochem.* **1973**, *46*, 421-426.

(48) Gibian, M. J.; Baumstark, A. L. The reduction of aromatic nitro and related compounds by dihydroflavins. *J. Org. Chem.* **1971**, *36*, 1389-1393.

(49) Bunton, C. A.; Rubin, R. J. Micellar catalysis of the benzidine rearrangement. *Tetrahedron Letters* **1975**, 1, 55-58.

(50) Hudlický, M. *Reductions in Organic Chemistry*; Ellis Horwood: Chichester, 1984.

(51) Lyons, R. E.; Smith, L. T. Die Reduktion von nitroverbindungen mit eisen und löslichen chloriden. *Chem. Ber.* **1927**, *60*, 173-182.

(52) Kamm, O.; Marvel, C. S. b-phenylhydroxylamine. In *Organic Syntheses*; Gillman, H., Ed.; Wiley: New York, 1932; Vol. 1; pp. 445-447.

(53) Haderlein, S. B.; Schwarzenbach, R. P. Abiotic reduction of nitroaromatic compounds in the subsurface. In *Biodegradation of Nitroaromatic Compounds*; Spain, J., Ed.; Plenum: New York, 1995; pp. 199-225.

(54) Weber, E. J.; Wolfe, N. L. Kinetic studies of the reduction of aromatic azo compounds in anaerobic sediment/water systems. *Environ. Toxicol. Chem.* **1987**, *6*, 911-919.

(55) Parris, G. E. Covalent binding of aromatic amines to humates. I. Reactions with carbonyls and quinones. *Environ. Sci. Technol.* **1980**, *14*, 1099-1106.

(56) Haderlein, S. B.; Schwarzenbach, R. P. Adsorption of substituted nitrobenzenes and nitrophenols to mineral surfaces. *Environ. Sci. Technol.* **1993**, *27*, 316-326.

(57) Palmer, C. D.; Cherry, J. A. Geochemical evolution of groundwater in sequences of sedimentary rocks. *J. Hydrol.* **1984/1985**, *75*, 27-65.

(58) Dunnivant, F. M.; Schwarzenbach, R. P.; Macalady, D. L. Reduction of substituted nitrobenzenes in aqueous solutions containing natural organic matter. *Environ. Sci. Technol.* **1992**, *26*, 2133-2141.

(59) Capellos, C.; Bielski, B. H. J. *Kinetic Systems: Mathematical Descriptions of Chemical Kinetics in Solution*; Wiley: New York, 1972.

(60) Wardman, P. The use of nitroaromatic compounds as hypoxic cell radiosensitizers. *Curr. Topics Rad. Res. Quart.* **1977**, *11*, 347-398.

(61) Banerjee, G.; Malhotra, S. N. Contribution to adsorption of aromatic amines on mild steel surface from HCl solutions by impedance, UV, and Raman spectroscopy. *Corrosion* **1992**, *48*, 10-15.

(62) Sherwood, T. K.; Pigford, R. L.; Wilke, C. R. *Mass Transfer*; McGraw Hill: New York, 1975.

(63) Laviron, E.; Vallat, A.; Meunier-Prest, R. The reduction mechanism of aromatic nitro compounds in aqueous medium. Part V. The reduction of nitrosobenzene between pH 0.4 and 13. *J. Electroanal. Chem.* **1994**, *379*, 427-435.

(64) Craig, B. D. *Fundamental Aspects of Corrosion Films in Corrosion Science*; Plenum: New York, 1990.

(65) Stratmann, M.; Bohnenkamp, K.; Engell, H.-J. An electrochemical study of phase-transitions in rust layers. *Corr. Sci.* **1983**, *23*, 969-985.

(66) Heijman, C. G.; Grieder, E.; Holliger, C.; Schwarzenbach, R. P. Reduction of nitroaromatic compounds coupled to microbial iron reduction in laboratory aquifer columns. *Environ. Sci. Technol.* **1995**, *29*, 775-783.

(67) Klausen, J. W.; Tröber, S. B.; Haderlein, S. B.; Schwarzenbach, R. P. Reduction of substituted nitrobenzenes in aqueous mineral oxide/Fe^{2+} suspensions. *Environ. Sci. Technol.* **1995**, submitted.

(68) Hubbard, A. T. Structure of the solid-liquid interface. In *Comprehensive Chemical Kinetics*; Elsevier, Amsterdam; Vol. 28, Reactions at the Solid-Liquid Interface: 1989; pp. 1-64.

(69) Kastening, B.; Holleck, L. Protonen- und elektronen-transfer an inhibitorbedeckten elektroden. *Electroanal. Chem. Interfac. Electrochem.* **1979**, *27*, 355-368.

(70) Laviron, E.; Meunier-Prest, R.; Lacasse, R. The reduction mechanism of aromatic nitro compounds in aqueous medium. Part IV. The reduction of p-nitrobenzo-phenone between H_0 = -5 and pH 14. *J. Electroanal. Chem.* **1994**, *375*, 263-274.

(71) Zuman, P.; Fijalek, Z.; Dumanovic, D.; Suznjevic, D. Polarographic and electrochemical studies of some aromatic and heterocyclic nitro compounds, Part I: General mechanistic aspects. *Electroanal.* **1992**, *4*, 783-794.

(72) Schwarzenbach, R. P.; Stierli, R.; Lanz, K.; Zeyer, J. Quinone and iron porphyrin mediated reduction of nitroaromatic compounds in homogeneous aqueous solution. *Environ. Sci. Technol.* **1990**, *24*, 1566-1574.

(73) Meites, L.; Zuman, P. *CRC Handbook Series in Organic Electrochemistry*; CRC: Cleveland, OH, 1979.

(74) *Dictionary of Organic Compounds;* 5th ed.; Chapman and Hall: New York, 1984.

(75) Perrin, D. D. *Dissociation Constants for Organic Bases in Aqueous Solutions*; Butterworths, England: 1965.

(76) Tucker, W. A.; Nelken, L. H. Diffusion coefficients in air and water. In *Handbook of Chemical Property Estimation Methods*; Lyman, W. J.; Reehl, W. F.; Rosenblatt, D. H., Eds.; McGraw Hill: New York, 1982; pp. 17.1-17.25.

(77) Smyth, M. R.; Osteryoung, J. G. A pulse polarographic investigation of parathion and some other nitro-containing pesticides. *Anal. Chim. Acta* **1978**, *96*, 335-344.

(78) Pankow, J. F. *Aquatic Chemical Concepts*; Lewis: Chelsea, MI, 1991.